Chen *et al. Carbon Research* (2023) 2:8
https://doi.org/10.1007/s44246-023-00041-9

Carbon Research

REVIEW

Open Access

Application of covalent organic frameworks and metal–organic frameworks nanomaterials in organic/inorganic pollutants removal from solutions through sorption-catalysis strategies

Zhongshan Chen[1], Yang Li[1], Yawen Cai[2], Suhua Wang[3], Baowei Hu[2], Bingfeng Li[4], Xiaodong Ding[5], Li Zhuang[1] and Xiangke Wang[1*]

Abstract

With the fast development of agriculture, industrialization and urbanization, large amounts of different (in)organic pollutants are inevitably discharged into the ecosystems. The efficient decontamination of the (in)organic contaminants is crucial to human health and ecosystem pollution remediation. Covalent organic frameworks (COFs) and metal–organic frameworks (MOFs) have attracted multidisciplinary research interests because of their outstanding physicochemical properties like high stability, large surface areas, high sorption capacity or catalytic activity. In this review, we summarized the recent works about the elimination/extraction of organic pollutants, heavy metal ions, and radionuclides by MOFs and COFs nanomaterials through the sorption-catalytic degradation for organic chemicals and sorption-catalytic reduction-precipitation-extraction for metals or radionuclides. The interactions between the (in) organic pollutants and COFs/MOFs nanomaterials at the molecular level were discussed from the density functional theory calculation and spectroscopy analysis. The sorption of organic chemicals was mainly dominated by electrostatic attraction, π-π interaction, surface complexation and H-bonding interaction, whereas the sorption of radionuclides and metal ions was mainly attributed to surface complexation, ion exchange, reduction and incorporation reactions. The porous structures, surface functional groups, and active sites were important for the sorption ability and selectivity. The doping or co-doping of metal/nonmetal, or the incorporation with other materials could change the visible light harvest and the generation/separation of electrons/holes (e^-/h^+) pairs, thereby enhanced the photocatalytic activity. The challenges for the possible application of COFs/MOFs nanomaterials in the elimination of pollutants from water were described in the end.

Handling Editor: Hailong Wang.

*Correspondence:
Xiangke Wang
xkwang@ncepu.edu.cn
Full list of author information is available at the end of the article

Highlights

1. Sorption of (in)organic pollutants by metal–organic frameworks/covalent organic frameworks nanomaterials was reviewed.
2. Photocatalytic degradation of organic pollutants by metal–organic frameworks/covalent organic frameworks was discussed.
3. Photocatalytic reduction of metal ions using metal–organic frameworks/covalent organic frameworks was described.
4. Electrocatalytic extraction of radionuclides using metal–organic frameworks/covalent organic frameworks was compared.
5. Challenges for real application of metal–organic frameworks/covalent organic frameworks was provided.

Keywords Covalent organic frameworks, Metal–organic frameworks, Sorption, Catalytic reduction/degradation, Environmental pollutants

1 Introduction

Environmental pollution is one of the most critical global challenges to the human society. With the fast development of urbanization, agriculture and industrialization, and the high requirement of human life quality, different kinds of organic chemicals such as antibiotics, pesticides, persistent organic pollutants (POPs), inorganic pollutants such as metal ions (Pb(II), Cd(II), As(III), Cr(VI), Hg(II) etc.) and radionuclides (^{235}U(VI), $^{99}TcO_4^-$, $^{129}I_2$, $^{137}Cs^+$, $^{90}Sr^{2+}$ and actinides etc.) in unclear energy utilization processes are inevitably discharged into the natural systems (Chen et al. 2022c; Huang et al. 2022; Liu et al. 2022e; Lu et al. 2022; Wang et al. 2022b). They are not easily degraded or removed from ecosystems and thereby exist in the environment for a long time. Such pollutants in the environments are toxicity to human health even at ultralow concentrations because they can enter human body and then accumulate in human body across the food chain. For example, the Cd(II) poisoning could cause the injuries to skeletal and renal function systems (Zhao et al. 2011), the Pb(II) poisoning could cause the damage to cardiovascular and cranial nerve systems (Rouhani and Morsali 2018). Meanwhile, the presence of organic chemicals in environment could also result in toxicity on nervous systems (Liu et al. 2021a). Thereby, it is critical to eliminate the pollutants to avoid the potential pollution to human ecosystems. Many methods such as membrane, adsorption, filtration, ion exchange, (co)precipitation, (photo)degradation, (photo)reduction, (electro)extraction and biological treatment have been investigated in the elimination of (in)organic pollutants from solutions (Chen et al. 2022a; Liu et al. 2022a; Wang et al. 2023; Xu and Tsang 2022; Yang et al. 2022; Zhang et al. 2022b; Zhu et al. 2022). These techniques for the removal of pollutants are generally dependent on the polluted water conditions such as the pollutant concentrations, coexisted pollutants, pH, temperature, etc. and the properties of the pollutant itself. Each technique has its advantages and disadvantages for real applications, which is normally related to the requirement of wastewater treatment and the species or structures of pollutants. More importantly, the structures and surface properties of the materials are most important parameters for the elimination of (in) organic contaminants (Yu et al. 2022; Zhang et al. 2022c). The nanomaterials have been studied extensively in pollution management because they have super advanced properties such as high surface areas, abundant active sites, porous structures, physical and chemical stability at extreme conditions and multifunctional groups for sorption-catalytic activities, etc. Mauter and Elimelech (2008) reviewed different carbon-based nanomaterials such as fullerene, carbon onion, carbon nanotubes and graphene for pollution treatment. The nanomaterials as adsorbents, membranes, filters and antimicrobial agents for the elimination and separation of (in)organic contaminants were described, and the authors concluded that the porous structures/sizes, surface functional groups and surface properties were critical for the selective and efficient removal of organic molecules and metal ions. Gupta and Saleh (2013) summarized the sorption of (in)organic pollutants from wastewater by carbon nanotubes, porous carbon materials and fullerene as adsorbents. The sorption of pollutants by the carbon materials was not only related to solution conditions such as pH, temperature, salt concentrations, but also dependent on the properties of pollutants and the nanomaterials such as species and microstructures of pollutants, surface charge, surface groups and active sites of materials etc.

Covalent organic frameworks (COFs) have well-defined crystal porous structures and are easily modified with functional groups, which offer the superior properties in multidisciplinary areas such as gas storage, catalysis, sorption and electricity etc. Ding and Wang (2013) reviewed the synthesis and application of COFs in gas

storage, photoelectricity and catalysis, and concluded that COFs were promising materials in future if they could be mass-produced at a low price. The H_2 storage, methane storage, ammonia storage, photoelectric and photocatalytic applications in pollution decontamination were summarized. Xu et al. (2022) reviewed the radionuclides removal by COFs, and found that COFs could selectively adsorb radionuclides if the pore sizes, skeletons and active sites could be precisely predesigned and constructed. Gu et al. (2022) reviewed the synthesis and application of COFs and COFs-based composites for the sorption and reduction of metals and radionuclides from solutions. The COFs could selectively remove target metals and radionuclides because the porous structures and the surface functional groups could form strong surface complexes and reduce the metals and radionuclides through redox reactions. More importantly, COFs could preconcentrate radionuclides through sorption-photocatalytic reduction processes to immobilize radionuclides in natural systems. Liu et al. (2021b) reviewed the different methods for COFs synthesis and modification of surface properties. The remediations of organic molecules and metal elements from solutions by COFs through sorption, precipitation and catalytic reduction/degradation were summarized and the interaction mechanisms of pollutant molecules with COFs were discussed from the viewpoint of advanced spectral techniques and computational simulation at molecular level. The authors concluded that COFs-based nanocomposites not only can adsorb organic molecules, but also can photocatalytically degrade organic chemicals under natural sunlight conditions because the COFs-based catalysts could absorb visible light and generate/separate the electrons/holes (e^-/h^+) pairs efficiently. For metal ions, the high valent metals adsorbed on COFs can also be reduced to low valent metals and thereby form precipitates on COFs or COFs-based materials.

Metal–organic frameworks (MOFs) with controlled pore sizes and structural tailorability are considered suitable materials for the remediation of pollutants from the natural environmental systems (Li et al. 2018a; Kitagawa 2014; Tchinsa et al. 2021). Li et al. (2009) summarized the gas purification and separation from the special properties of MOFs. The distinguished special properties of MOFs such as the adjustable pore structures and sizes, large surface areas and thermal chemical stability, assured the separation of gases from their molecule structures. Czaja et al. (2009) discussed the possible industrial application of MOFs in the areas of gas storage, separation and purification, and the heterogeneous catalysis of organic molecules. Liu et al. (2022b) summarized the different strategies for MOFs synthesis and their applications in energy conversion, gas storage and pollutants' remediation. The authors found that the doping of single metals could enhance the photogeneration of the active free species radicals and improve the degradation of the organic molecules or reduction of metal ions. The porous structures, surface group modification and metal oxide-loading are efficient methods to improve the sorption and catalytic activities of MOFs. Zhang et al. (2022d) reviewed the synthesis and functionalization of COFs and MOFs, and their applications in hydrogen generation, carbon dioxide reduction and pollutants' remediation. The interaction of organic molecules with the nanomaterials was mainly dominated by H-bonding, electrostatic attention, π-π interaction, and surface complexation. The removal efficiency of metal ions was affected by the conditions of solution such as pH, temperature, ionic strength, etc., and the properties of MOFs/COFs such as surface functional groups, active sites and doping/co-doping of metals/nonmetals and metal oxides. The binding of (in)organic contaminants was affected by the porous structures, inner pore sizes, and surface groups. The MOFs and COFs can not only adsorb the (in)organic contaminants, but also degrade organic molecules or reduce the metal ions under natural sunlight conditions. The shape and size selectivity, and the enhanced catalytic activity provided the potential possibility of bare MOFs or MOF-based composites in chemical industries' applications.

From the abovementioned results, one can see that MOFs and COFs have been extensively studied in the separation and purification of gases, in the removal of (in) organic contaminants through sorption and catalysis strategies. However, the review for the decontamination of pollutants and selective extraction of target elements still has not been fully discussed, especially the mechanism discussion at the molecular level from the advanced spectroscopic measurements and computational simulation together with batch and column experimental results is still not available. In this review, the authors mainly summarized the decontamination of organic/inorganic pollutants, the in-situ immobilization and selective separation of target metals or radionuclides from complicated systems. The mechanism was discussed and the challenges for potential applications were described in the end.

2 Synthesis of MOFs and COFs nanomaterials

Yaghi's group for the first time synthesized COFs through condensation reaction. The crystal structure was formed by strong bonds among C, O and B atoms with the inner pore sizes of 7–27 angstroms, with high thermal stability, high surface area and porosity (Cote et al. 2005). The authors used simple "one-pot" process under mild

condition. From molecular dehydration reaction, three $C_6H_5B(OH)_2$ was converged to form B_3O_3 ring. The cyclotrimerized boronic acids were then reacted with 1,4-benzenediboronic acid for 74 h at 120 oC in mesitylene-dioxane solution to form COFs-1. Since then, the COFs had been synthesized by different techniques such as microwave technique (Ren et al. 2012), sonochemical technique (Tuziuti et al. 2008), ionothermal technique (Maschita et al. 2020), mechanochemical technique (Biswal et al. 2013), solvothermal technique (Guo et al. 2021), etc. Hao et al. (2023) synthesized COFs by the addition of 5,5'-(diazene-1,2-diyl)bis(2-aminobenzonitrile), 4,4'-(thiazolo[5,4-d]thiazole-2,5-diyl)dianiline and 2,4,6-triformylphloroglucinol in orthodichlorobenzene/n-butanol/acetic acid (volume ratio of 5:5:1) mixture solution. The solution was frozen in N_2 liquid bath and then heated at 120 °C for 3 days, and thus achieved the COF-1 nanomaterial. Feng et al. (2012) summarized the synthesis of COFs and concluded that geometry retention, building block diversity and covalent reaction reversibility were the three critical factors, which affected the design and synthesis of COFs. According to the requirement, the COFs could be designed using different chemicals under different conditions. The pore sizes and porosities could be adjusted, which is important for the special applications of COFs and COF-based nanomaterials.

MOFs was also for the first time reported by Yaghi's group (Yaghi et al. 1995). They synthesized MOFs with microporous structures by diffusion method and applied for aromatic molecules capture selectively. They used the symmetry of starting building molecular to react with metals for the covalent solid formation with open framework. The 1,3,5-benzenerricarboxylate and $Co(NO_3)_2$ were mixed in alcohol for 3 days to achieve the pink and cubic crystals, which were stable in water and organic solvents. The XRD analysis revealed the structure of $CoC_6H_3(COOH_{1/3})_3(NC_5H_5)_2{\cdot}2/3NC_5H_5$. Zhou and Kitagawa (2014) summarized the MOFs synthesis methods, which were classified as: coordination-bonding or metal-containing node; post-modification of ligands; and symmetry-assistant synthesis. The doping of metal clusters could significantly improve the MOFs stability and porosity. The cation exchange at metal-containing nodes could construct the conceptual framework to form metal–ligand bond cleavage. The functional groups could be attached on MOFs by pre-synthetic or post-synthetic modification. The MOFs can be applied in energy transfer, CO_2 reduction, H_2 generation and storage, photocatalysis degradation of organic molecules, photoreduction-immobilization of metal ions (Barea et al. 2014; Canivet et al. 2014; Voorde et al. 2014; Zhang and Lin 2014).

The properties of MOFs and COFs synthesized under different conditions using different techniques are different. The synthesis methods, the surface areas, pore volumes, pore sizes, crystal structures and zeta potential values of MOFs and COFs synthesized under different conditions are tabulated in Tables 1 and 2. The synthesis of MOFs and COFs nanomaterials have been reported and summarized extensively. The price for the synthesis of MOFs and COFs, their application for U(VI) extraction are summarized in Table 3. From the values in Table 3, one can see that the price for MOFs or COFs synthesis is relatively higher than that of most commercial carbon materials such as active carbon and biochar materials. However, the high sorption ability and reusability of MOFs and COFs will decrease the relative cost of MOFs and COFs in possible applications. The main purpose of this review is the usage of MOFs and COFs nanomaterials in the remediation of organic pollutants, metals and radionuclides. Thereby, the synthesis of these nanomaterials was not summarized in detail in this work. From the web of science knowledge, the key research points about the synthesis of MOFs and COFs, and the application in the remediation of environmental (in)organic pollutants are given in Fig. 1 (Chen et al. 2019; Cote et al. 2005; Mahata et al. 2006; Niu et al. 2014; Shen et al. 2013; Yaghi et al. 1995).

3 Organic pollution treatment

The organic contaminants mainly include dyes, antibiotics and other organic chemicals produced in the chemical industry processes. The organic pollutants could be eliminated by MOFs and COFs nanomaterials through adsorption, photocatalytic degradation, chemical and biological treatments. In this section, the adsorption and photocatalytic degradation of organic chemicals using COFs and MOFs nanomaterials as adsorbents or catalysts were mainly discussed.

3.1 Adsorption

Yuan et al. (2019) summarized the preparation of COF membranes and their application for dye separation in wastewater treatment. Through adjusting the tunable porous structures and inner sizes, the functionality and hydrophobicity/hydrophilicity, the dyes could be separated from wastewater efficiently. The sorption of antibiotics on the nanomaterials was dependent on the nanomaterial surface properties and porous structures (Ahmed et al. 2015). Kong et al. (2022) prepared COP-NH_2, which had flexible hydrophobic triptycene and multi-amines. The sorption of dichromate and perfluorooctane sulfonate (PFOS) showed the sorption capacities of 1.4 mmol/g for PFOS and 3.5 mg/g for dichromate. The high sorption capacity was mainly

Table 1 The properties of the COFs materials

COFs	Synthesis method	Critical parameters	BET surface (m^2/g)	Pore volume (cm^3/g)	Pore size	Zeta potential	Crystal structure	Ref
PS-COF-1	solvothermal	80°, 72 h	2703	2.68	~4.5 nm	-	2D layered crystal	Hao et al. (2022a)
o-GS-COF	solvothermal	120°, 12 h	51.5	-	-	-	2D layered crystal	Wen et al. (2018)
COF-HAP	solvothermal	120°, 72 h	26.9	0.14	15 Å	-	crystalline	You et al. (2020)
COF-HHTF-AO	solvothermal and amidoximation	120° for 72 h, and then amidoximation at 70°	275	-	0.2 nm	1.3	2D layered crystal	Cheng et al. (2021)
TaTp-1 COF/CDs	hydrothermal	room temperature	76	-	2.59 nm	-	Core–shell, 2D layered crystal	Qin et al. (2022)
TAPB-BMTTPA-COF	solvothermal and in situ growth	120°, 72 h	1934	1.03	3.2 nm	-	Core–shell, 2D layered crystal	Huang et al. (2017)
Fe_3O_4/TpPa-1	solvothermal	120°, 72 h	485.2	0.34	2 nm	-	Core–shell, 2D layered crystal	Zhong et al. (2020)
TpPa-1	solvothermal	120°, 72 h	688.8	0.42	2 nm	5.63	2D layered crystal	Zhong et al. (2020)
Fe^0/TpPa-1@DOPA	solvothermal	120°, 72 h	103	-	20.234 Å	3.9	-	Shen et al. (2022)
AO-COF-ben	solvothermal	120°,72 h,Amidoximated by treatment with hydroxylamine	218	0.16	12.8 Å	-	2D layered structure	Chen et al. (2022b)
AO-COF-tri	solvothermal	120°,72 h,Amidoximated by treatment with hydroxylamine	203	0.17	21.3 Å	-	2D layered structure	Chen et al. (2022b)
COF@PDA	high-temperature condensation polymerization	180°, 72 h	118.2	-	-	-	Core–shell structure, amorphous	Xiao et al. (2021)
SCU-COF-2	solvothermal	120°, 72 h	413.4	-	-	-	2D layered crystal	He et al. (2021)
COF/GO	solvothermal	120°, 24 h	179	0.24	1.36 nm	- 39.3 mV	3D macroporous structure	Li et al. (2022a, b, c)
Fe_3O_4@COFs	in situ growth	room temperature	55.7	0.12	-	-	Core–shell structure	Li et al. (2019)
FeOOH@Tz-COF	solvothermal	30°, 72 h, and then In situ growth core–shell structure	892	-	1.4	-	Core–shell structure	Guillem-Navajas et al. (2022)

dominated by the amine protonation and electrostatic reaction, which resulted in the simultaneous high removal efficiency of > 99% in electroplating wastewater. Wang et al. (2022a) prepared OH-rich COFs and used them for the adsorption of azo dyes like eriochrome black T (EBT), congo red (CR) and eriochrome blue R (EBR) from solutions. The COF-OH exhibited the sorption capacities of the three dyes ranging from 91 to 229 mg/g with the removal efficiency > 76%. The difference in the sorption of the three dyes was described in detail. However, the reason and interaction mechanism for the sorption difference of three dyes were not investigated and discussed in detail in this work. The steam activation, chemical activation, alkali treatment, or acidic treatment could improve the surface functionalities, porous structures, and active sites, and thereby could enhance the sorption abilities of different organic contaminants from wastewater (Ahmed et al. 2016). Wang et al. (2013) reviewed the sorption of pollutants in wastewater treatment and concluded that the surface strong acidity and abundant functional groups of nanomaterials could bind pollutants through surface complexation and strong π-π reaction. The loading of graphene in porous nanomaterials is a promising method to enhance the sorption ability of environmental pollutants in wastewater decontamination.

Table 2 The properties of the MOFs materials

MOFs	Synthesis method	Critical parameters	BET (m^2/g)	Pore volume cm^3/g	Pore size (nm)	Crystal structure	Ref
ZJU-X11	solvothermal	95°, 24 h	-	-	-	Cationic monoclinic	Kang et al. (2021)
SCU-103	solvothermal	140°, 72 h	-	-	-	-	Shen et al. (2020)
UiO-66-QU	solvothermal	130°, 48 h	83.27	0.166	7.98	crystalline and cubic skeleton structure	Hu et al. (2023b)
MOFL-TpBD	solvothermal	120°, 1 h	535	-	1.5	2D layered crystal	Li et al. (2021c)
MFC-N	hydrothermal	110°	722	0.42	4.1	Core–shell structure, Crystal	Huang et al. (2018)
Fe_3O_4@MIL-101(Cr)	solvothermal	210°,8 h, in situ synthesis	2270	1.04	-	Core–shell, truncated octahedral morphology	Folens et al. (2016)
Fe_3O_4@MIL-101(Cr)	solvothermal	210°,8 h, in situ synthesis	2270	1.04	-	Core–shell, truncated octahedral morphology	Folens et al. (2016)
MFC-N	hydrothermal	110°	722	0.42	4.1	Core–shell structure, Crystal	Huang et al. (2018)
MFC-O	hydrothermal	110°	782	0.47	3.8	Core–shell structure, Crystal	Huang et al. (2018)
GO–COOH/UiO-66	solvothermal	100°, 8 h	731.08	0.17	1.30	Crystal structure	Yang et al. (2017)

Table 3 Cost estimation for preparing the materials and for applying U extraction from seawater

Materials	Cost estimation for preparing the materials	Cost estimation for U extraction from seawater	Ref
MOF-NH_2	\$150/kg	-	Gong et al. (2021)
MOF-OH	\$150/kg	-	Gong et al. (2021)
PS-COF-1	~\$64,500/kg	-	Hao et al. (2022a)
MoO_3-biochar	\$1/kg	-	Li et al. (2022a, b, c)
commercial activated carbon	\$1.8–3.9/kg	-	Li et al. (2022a, b, c)
ion exchange resin	\$9–15.7/kg	-	Li et al. (2022a)
In — Nx — C — R	\$41,000/kg	\$806/kg U	Liu et al. (2022d)
TpPa-1	\$7520/kg	-	Karak et al. (2017)
Land uranium reserves	-	\$100–335/kg U	Li et al. (2020)
PAF-170-AO	-	\$189.77/kg U	Li et al. (2020)

Li et al. (2022c) constructed ultrathin COFs on graphene (GO) to prepare COF/GO composites with 3D macroporous structures (1.36 nm) and excellent-exposed sorption sites, which permitted the rapid diffusion and sorption of organic pollutants (i.e., methylene blue (MB), Rhodamine B (RhB) and crystal violet (CV)) from solutions. Due to the macroporous channels, the organic pollutant molecules could diffuse into the channels rapidly, thereby the COF/GO showed rapid removal kinetics of organic molecules. However, the COFs only allowed the MB (the molecule size smaller than the pore size) to enter into the COF channel, whereas the dyes with large molecule sizes (RhB and CV) were rejected to enter into COF channel and could only be adsorbed on the crystallite surface (Fig. 2a). However, the ultrathin COFs provided abundant sorption sites and thereby exhibited high sorption capacities for the dyes (Fig. 2b). The COF/GO composites exhibited the sorption capacities of 328 mg/g for CV, 334 mg/g for MB and 368 mg/g for RhB, which were much higher than the bulk COFs (178 mg/g for CV, 308 mg/g for MB and 130 mg/g for RhB). The ultrathin COF/GO could extremely shorten the reaction time to achieve the sorption equilibration (Fig. 2c) and the sorption capacity was about 3 times higher than that of COFs (Fig. 2d). DFT calculation showed that the RhB interacted with COFs to form N–H···Cl H-bond (H-bond energy of -6.69 kcal/mol) through H atom to N atom of COFs with Cl^- atom of RhB, and form S–O···H H-bond

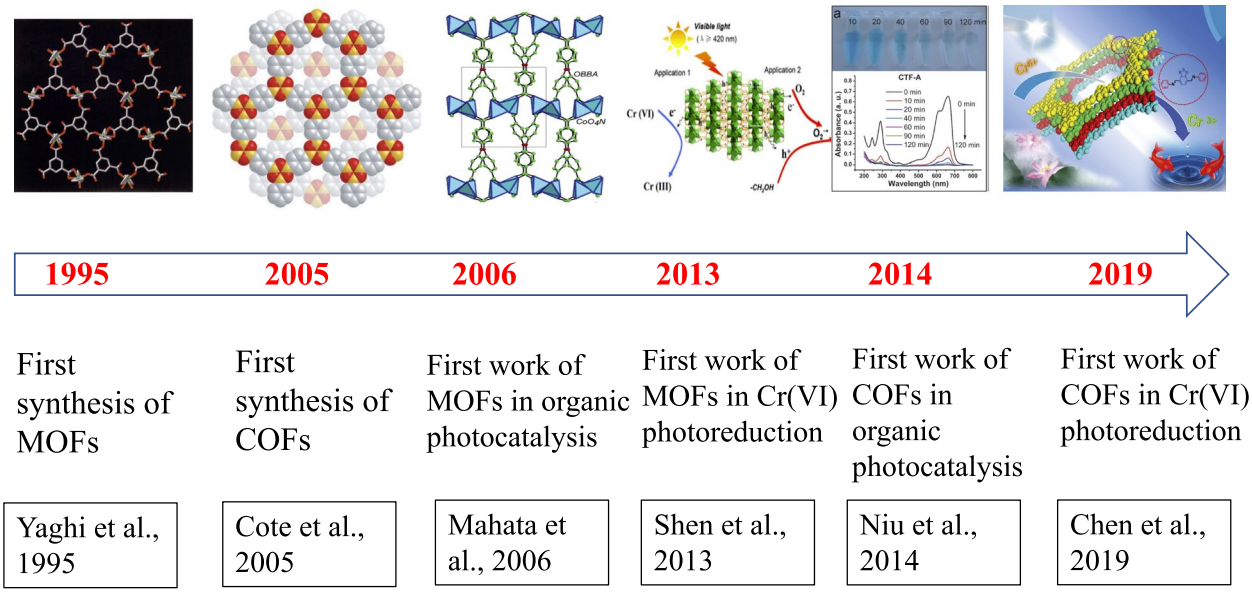

Fig. 1 The synthesis and application of MOFs and COFs

(H-bond energy of -12.01 kcal/mol) through O atom of $-SO_3$ of COFs and H atom of –COOH in RhB. The DFT calculation also indicated that electrostatic interaction, H-bond, π-π interaction contributed to the RhB sorption on COF/GO composites.

Muslim et al. (2022) synthesized bifunctional MOFs materials for the sorption of methylene blue (MB) and methyl orange (MO) from wastewater, and achieved the sorption capacities of 116 mg/g for MB and 103 mg/g for MO. The anionic and cationic dyes could be simultaneously removed from solutions, which was attributed to the non-covalent reactions of dyes with the porous materials. Huang et al. (2018) investigated the removal abilities of metal ions and dyes from wastewater by Zr-MOFs. The amine-loaded MOFs had the sorption capacities of 102 mg/g for Pb(II), 128 mg/g for MB and 219 mg/g for MO. Different types of dyes could be selectively separated from complex solutions through adjusting solution pH. The adsorption mechanisms were generally attributed to cationic and ionic exchange, electrostatic interaction, H-bonding, pore filling, n-π and π-π interaction (Tran et al. 2017; 2020). If the adsorption was affected by pH and ionic strength obviously, electrostatic attraction would play primary role in the adsorption process. The reversible adsorption–desorption could be attributed to cationic or ionic exchange, whereas irreversible adsorption–desorption could rule out the cationic or ionic exchange mechanism. The -OH peak shifting in FTIR before and after adsorption could provide some information of H-bonding interaction. The n-π interaction could be derived from the C-O peak shifting in FTIR before and after adsorption, whereas the π-π interaction could be derived from the FTIR analysis if the C=C peak intensity decreased and upshifted after adsorption. The decrease of S_{BET} and V_{total} after adsorption suggested the possibility of pore filling mechanism. From the above-mentioned results, it is clear that the COFs or MOFs nanomaterials showed very high sorption capacities for organic contaminants from wastewater. The selectivity of target organic molecules in the presence of different organic pollutants with different molecular structures was relatively weak, which was mainly due to the functional groups on porous structures of nanomaterials and the organic molecule structures. Without special functional groups and tunable porous structures, the MOFs or COFs nanomaterials could adsorb the organic molecules with high sorption capacity, but the selectivity was weak. The surface special functional groups, active sites and tunable porous structures could improve the binding of special organic molecules, thereby improved the sorption selectivity.

3.2 Photocatalytic degradation

Besides the elimination of organic molecules through sorption process, the photocatalytic degradation can also degrade organic pollutants efficiently, especially at low concentrations under complicated systems. Wang et al. (2020a) reviewed and compared the synthesis of B-containing and N-containing COFs. The structures and morphologies of COFs could be easily adjusted through controlling different reaction conditions and synthesis methods. The effect of porous structures and morphologies of COFs on the photocatalytic decontamination of organic contaminants was discussed in detail. The authors concluded that the π-stacking interlayer

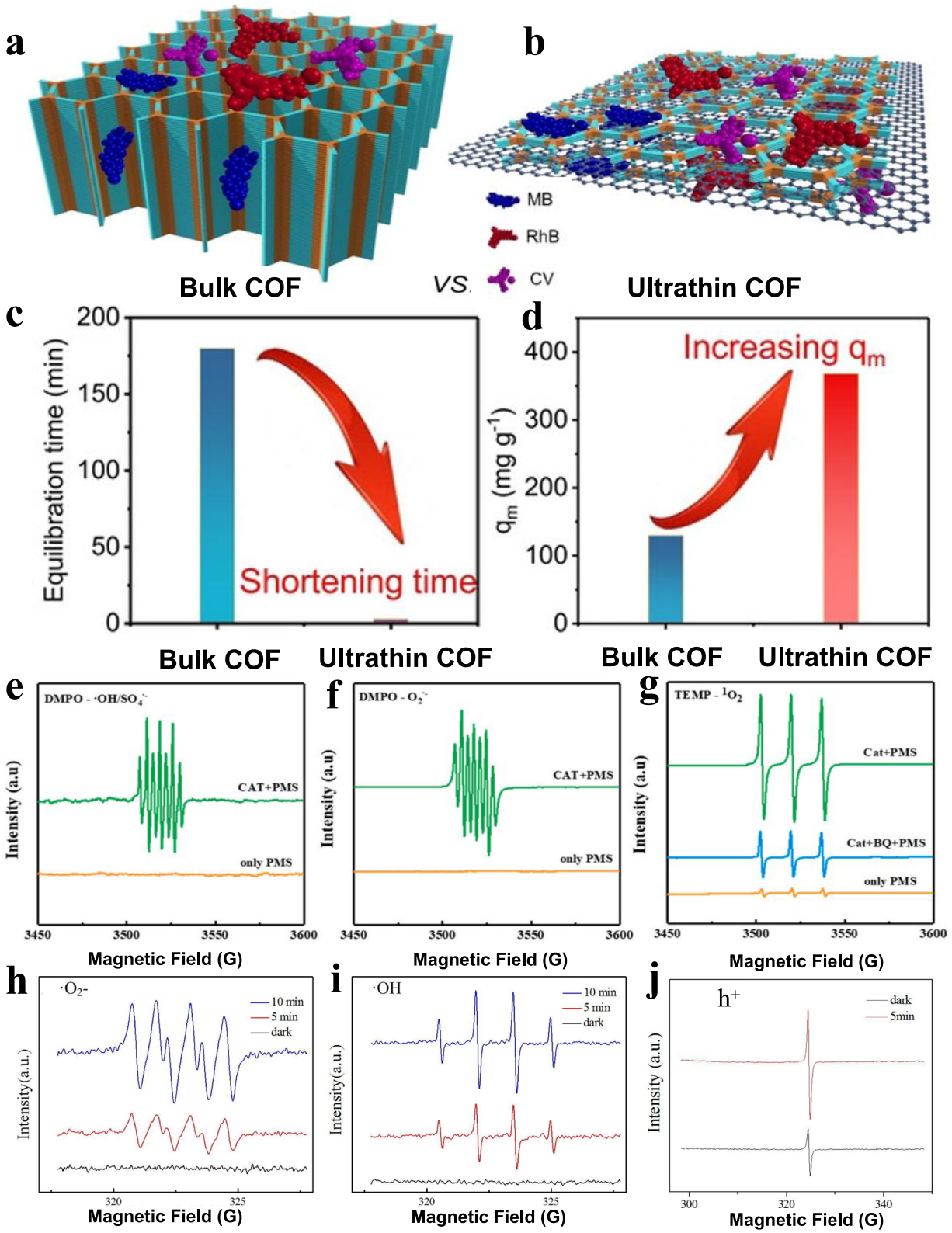

Fig. 2 Diffusion and surface adsorption of MB, RhB and CV on bulk COFs (**a**) and ultrathin COFs (**b**); The reaction time was shortened to achieve the sorption equilibration (**c**) and sorption capacity increased on ultrathin COFs (**d**) (Li et al. 2022a). ESR spectra of DMPO-$^{\bullet}$OH/$SO_4^{\bullet-}$ (**e**), DMPO-$O_2^{\bullet-}$ (**f**) and TEMP-$^1O_2$ signals (**g**) in Co-doped COFs (Cao et al. 2022); ESR spectra of DMPO-$O_2^{\bullet-}$ (**h**), DMPO-$^{\bullet}$OH (**i**) and TEMPO-$h.^+$ (**j**) in Fe-based MOFs in dark and visible light conditions (Wang et al. 2018)

structures exhibited high light absorption and excellent charge carriers transfer, which enhanced the photocatalytic activity for organic molecules degradation. Cao et al. (2022) prepared Co-doped COFs with Co-Nx sites, which exhibited high catalytic ability in the removal of levofloxacin (> 94%) in 2 h for peroxymonosulfate (PMS) activation. The Co-doped COFs had high stability and recycle ability in a wide pH range from 3 to 9. The electron spin resonance (ESR) technique was applied to verify the formation and contribution of reactive oxygen species (ROSs). The 2,2,6,6-tetramethyl-4-piperidinol (TEMP) and 5,5-dimethyl-1-pyrroline (DMPO) were used as trapping agents to capture singlet oxygen ($^1O_2$) active species and short lifetime radicals, respectively. With only PMS, no DMPO-$O_2^{\bullet-}$ and DMPO-$^{\bullet}OH/SO_4^{\bullet-}$ was observed. The oxidation of DMPO by reactive oxygen species (ROSs) generated hydroxyl radial ($^{\bullet}OH$) and $SO_4^{\bullet-}$ species (Fig. 2e). The strong signal of DMPO-$O_2^{\bullet-}$ indicated the formation of superoxide radial ($O_2^{\bullet-}$) active species (Fig. 2f). The strong TEMP-$^1O_2$ signal suggested the formation of $^1O_2$ species. However, the addition of benzoquinone (BQ) for the quenching of $O_2^{\bullet-}$ active species showed the weaken of the signal, suggesting the generation of $^1O_2$ was related to $O_2^{\bullet-}$ active species (Fig. 2g). The Co-Nx sites and C = O groups were favorable for the generation of $^1O_2$, $O_2^{\bullet-}$ and $^{\bullet}OH$ free radicals, which were the main active species for levofloxacin degradation. The metal-doping and introduction of surface groups on COFs are efficient methods to improve the catalytic ability of COFs in the photo-degradation of organic molecules. Tan et al. (2016) found that the abundant functional groups, porous structures, and active sites could enhance the photogeneration and e^-/h^+ separation, which was helpful to construct the catalysts with enhanced photocatalytic activity in organic contaminants' degradation. The electrostatic attraction, π-π interaction, surface complexation and H-bonding interaction were important sorption mechanisms for the removal of organic molecules from wastewater to nanomaterials. The Fe-based MOFs were applied for the photocatalytic degradation of tetracycline (TC) and the Fe-based MOFs exhibited the removal efficiency of 96% at TC initial concentration of 50 mg/L. The ESR analysis showed no $O_2^{\bullet-}$ signal in dark, and DMPO-$O_2^{\bullet-}$ signal was detected under visible light conditions (Fig. 2h). No $^{\bullet}OH$ signal was found in dark. The DMPO-$^{\bullet}OH$ signal was detected under visible light condition, and the peak intensity enhanced with the increase of irradiation time (Fig. 2i). The similar results for 2,2,6,6-Tetramethylpiperidine 1-oxyl-h^+ (TEMPO-h^+) signals were also achieved (Fig. 2j). The results revealed that $O_2^{\bullet-}$, $^{\bullet}OH$ and h^+ active species contributed to TC photocatalytic degradation, which was in good agreement with quenching experimental results (Wang et al. 2018). The removal mechanism and sorption abilities of different organic pollutants by different kinds of MOFs and COFs nanomaterials, and comparison with carbon nanomaterials, are summarized in Table 4. The applications of MOF-based composites for the removal of organic pollutants were reviewed (Wang et al. 2020b), and the authors summarized that the carbon material incorporated MOFs, metal-doped MOFs, COFs/MOFs composites, and semiconductor incorporated MOFs had higher visible light harvest, generation and separation of e^-/h^+ pairs, higher stability and excellent reusability. The MOFs-based composites showed more practical applications in organic contaminants adsorption and photocatalytic degradation.

4 Heavy metal pollution treatment

Heavy metals such as Pb(II), As(III), Cr(VI), Zn(II), Cd(II), Hg(II), Cu(II), are released to the environment with the rapid development of industrialization, mining activities and municipal engineering. The metal ions are persisted in rivers, lakes or groundwaters for a long time and are impossible to be degraded without human initiatives. They could be accumulated in the living creatures, and result in serious human health risks (Zahed et al. 2021; Zaynab et al. 2022). Thereby, it is important to eliminate the heavy metal ions from eco-systems. The sorption method is efficient to remove the metal ions from water. However, the in-situ precipitation and immobilization are more efficient to reduce the toxicity and mobilization of heavy metals for very complicated conditions. In this section, we described the recent works for the sorption and photocatalytic reduction-precipitation of metals using MOFs and COFs nanomaterials.

4.1 Sorption of metal ions

Sorption of metal ions from wastewater is widely used in wastewater treatment because of its easy operation on large scale. Ding et al. (2016) constructed thioether-functional COFs for the selective detection/removal of Hg(II) ions in wastewater. The COFs exhibited high removal efficiency of Hg(II) with high selectivity and excellent sensitivity. The high selective and strong interaction of Hg(II) with COFs were dominated by the formation of Hg-thioether complexes, which highlighted the application of COFs for the simultaneous fluorescence sensing and elimination of Hg(II) ions in environmental pollution treatment. Huang et al. (2017) synthesized stable COFs through structural skeleton adjusting, pore walls, porous sizes, mesopores and high specific surface areas, which had high stability in strong basic or acidic solutions. The prepared COFs showed high efficiency, selectivity, effectivity and reusability removal of Hg(II), which offered a molecule platform for the removal of target metal ions

Table 4 Summary of Langmuir maximum adsorption capacity and the related interaction/degradation mechanisms

Materials categories	Name	Application	Maximum adsorption capacity (mg/g)	pH	Co range (ppm)	Temperature	Interaction or degradation mechanism	Ref
COF	PS-COF-1	$ReO_4/^{99}TcO_4$	1262	6	0 -800	298 K	Anion exchange, electrostatic interaction	Hao et al. (2022a)
MOF	ZJU-X11	$ReO_4/^{99}TcO_4$	518	-	100–536	298 K	Anion-Exchange	Kang et al. (2021)
MOF	SCU-103	$ReO_4/^{99}TcO_4$	318	7	5–400	298 K	Anion-Exchange	Shen et al. (2020)
COF	o-GS-COF	U(VI)	144.2	4.5	0–220.1	298 K	Oxygen atoms coordination interactions	Wen et al. (2018)
COF	COF-HAP	U(VI)	392.2	3	0.25–1000	298 K	Surface precipitate, surface complexation, and ion exchange	You et al. (2020)
COF	COF-HHTF-AO	U(VI)	550.1	6	0–100	298 K	Coordination interaction	Cheng et al. (2021)
Biochar	BC@LDH@HAP	Eu(III)	714	6	60–140	318 K	Surface complexation, ion exchange, and precipitation	Dong et al. (2021)
MOF	UiO-66-QU	Hg(II)	556	3	100–600	298 K	Monolayer chemical adsorption	Hu et al. (2023b)
COF	TaTp-1 COF/CDs	Hg(II)	235	7	0.01–0.15	298 K	Affinity for nitrogen and oxygen atoms	Qin et al. (2022)
Biochar	BMS-biochar	Hg(II)	320.1	7	1.0–25	298 K	Surface adsorption, electrostatic attraction, surface adsorption, and electrostatic attraction	Lyu et al. (2020)
Biochar	HCB	Hg(II)	5	-	0.1–5	298 K	C = C and C = O induced Hg-πbinding	Xu et al. (2016)
COF	TAPB-BMTTPA-COF	Hg(II)	734	7	-	298 K	Pore filling, coordination interactions, charge-transfer interaction	Huang et al. (2017)
COF	Fe_3O_4/TpPa-1	Cr(VI)	245.5	1	-	298 K	Hydrogen -bonding and π-π interaction, occupied in the pore cages	Zhong et al. (2020)
COF	TpPa-1	Cr(VI)	310.8	1	-	298 K	Hydrogen -bonding and π-π interaction, occupied in the pore cages	Zhong et al. (2020)
COF	Fe^0/TpPa-1@DOPA	Cr(VI)	516	2.6	20–80	298 K	Electrostatic adsorption, reduction, and coprecipitation	Shen et al. (2022)
Biochar	BC@EDTA-LDH	Cr(VI)	52.22	3	20–250	300 K	Surface adsorption and interlayer anion exchanges	Huang et al. (2019)
Biochar	MMABC	Cr(VI)	25.3	3	5–200	298 K	Adsorption-reduction-adsorption	Zhang et al. (2018)
Biochar	ZnO/ZnS modified biochar	Cr(VI)	24.5	6	5–400	298 K	Complex with hydroxyl groups	Li et al. (2018b)
MOF	MOFL-TpBD	Pb(II)	21.7	6	0.05–50	298 K	Chemisorption	Li et al. (2021c)
Biochar	ZnO/ZnS modified biochar	Pb(II)	135.8	6	5–400	298 K	Complex with hydroxyl groups	Li et al. (2018b)

Table 4 (continued)

Materials categories	Name	Application	Maximum adsorption capacity (mg/g)	pH	Co range (ppm)	Temperature	Interaction or degradation mechanism	Ref
Biochar	MoO_3-biochar	Pb(II)	229.87	4	5–120	298 K	Surface electrostatic attraction, ion exchange and surface complexation	Li et al. (2022b)
MOF	MFC-N	Pb(II)	102	6	-	298 K	Chelating	Huang et al. (2018)
MOF	Fe_3O_4@MIL-101(Cr)	As(III)	121.5	7	-	298 K	Redox reactions and binding on terephthalate ligands	Folens et al. (2016)
MOF	Fe_3O_4@MIL-101(Cr)	As(V)	80	7	-	298 K	Redox reactions and binding on terephthalate ligands	Folens et al. (2016)
COF	AO-COF-ben	ROX	732	4	-	298 K	Intermolecular hydrogen bonding and π-π electron donor–acceptor interactions	Chen et al. (2022b)
COF	AO-COF-tri	ROX	787	4	-	298 K	Intermolecular hydrogen bonding and π-π electron donor–acceptor interactions	Chen et al. (2022b)
Biochar	BC-450	Ni(II)	24.8	8.3	50–400	298 K	Surface complexation	Amin and Chetpattananondh (2019)
COF	COF@PDA	Ni(II)	207.5	6	-	303 K	Phenolic hydroxyl groups participate	Xiao et al. (2021)
Biochar	ZnO/ZnS modified biochar	Cu(II)	91.2	6	5–400	298 K	Complex with hydroxyl groups	Li et al. (2018b)
COF	COF@PDA	Fe(II)	204.9	6	-	303 K	Phenolic hydroxyl groups participate	Xiao et al. (2021)
COF	COF@PDA	Co(II)	194.2	6	-	303 K	Phenolic hydroxyl groups participate	Xiao et al. (2021)
COF	SCU-COF-2	CH_3I	1450	-	-	298 K	Charge conversion, anion-exchange	He et al. (2021)
COF	SCU-COF-2	I_2	6000	-	-	298 K	Eactive pyridine nitrogen atoms	He et al. (2021)
COF	COF/GO	MB	328	-	20–900	298 K	Electrostatic interaction, H-bond, π-π interaction	Li et al. (2022a, b, c)
COF	COF/GO	CV	334	-	20–900	298 K	Electrostatic interaction, H-bond, π-π interaction	Li et al. (2022a, b, c)
COF	COF/GO	RhB	368	-	20–900	298 K	Electrostatic interaction, H-bond, π-π interaction	Li et al. (2022a, b, c)
COF	Fe_3O_4/TpPa-1	BPA	1220.97	6	-	298 K	Hydrogen -bonding and π-π interaction, occupied in the pore cages	Zhong et al. (2020)
COF	TpPa-1	BPA	1424.27	6	-	298 K	Hydrogen -bonding and π-π interaction, occupied in the pore cages	Zhong et al. (2020)

Table 4 (continued)

Materials categories	Name	Application	Maximum adsorption capacity (mg/g)	pH	Co range (ppm)	Temperature	Interaction or degradation mechanism	Ref
COF	Fe_3O_4@COFs	TCS	5481	7	250–2000	298 K	Space embedding effect, van der Waals forces, and benzene ring π—π stacking	Li et al. (2019)
COF	Fe_3O_4@COFs	TCC	2085	7	125–2000	298 K	Space embedding effect, van der Waals forces, and benzene ring π—π stacking	Li et al. (2019)
MOF	MFC-N	MB	128	11	-	298 K	Electrostatic and p-p stacking interaction	Huang et al. (2018)
MOF	MFC-O	MO	219	3	-	298 K	Electrostatic and p-p stacking interaction	Huang et al. (2018)
COF	FeOOH@Tz-COF	As(III)	272	7	0.5–120	303 K	Multilayer sorption	Guillem-Navajas et al. (2022)

from solutions. Hussain et al. (2022) synthesized thiourea-based COFs, which had enol and keto tautomeric structures. The prepared COFs exhibited ultrahigh Hg(II) adsorption capacity (> 4200 mg/g) owing to the large amounts of chelating available sites. More importantly, the COFs were very stable with high removal efficiency and high selectivity in strong acidic solutions (1–3 mol/L HCl). The high selectivity of Hg(II) removal over other competing metals was attributed to the soft–soft reactions of Hg(II) ions with sulfur in COFs. Zhao et al. (2022) prepared bipyridine-based 2D COFs and applied them for Pd(II) elimination from aqueous solution. The COFs exhibited high selectivity and excellent sorption efficiency, with high selectivity of 92% and the sorption capacity of 532 mg/g. The theoretical calculation showed that the coordination of oxygen and pyridine nitrogen with Pd(II) was the main adsorption process. Li et al. (2022a) constructed COFs with -SO_3H functional groups, which had high porosity and crystallinity. The material exhibited high removal efficiency for multiple metal ions, such as Cr(III), Cd(II) and Fe(III) ions from complex solutions. The synergistic effect of crystallinity and -SO_3H functionalization contributed to the high sorption of metal ions. However, the selectivity of the COFs for target materials was not reported in this work. Jin et al. (2022) prepared O,N-rich COFs, which had large porphyrin center space and enough coordination sites. The O,N-rich COFs had high sorption of Cd(II) ions with excellent stability and reusability. The reaction of Cd(II) with porphyrin ring promoted the binding of Cd(II) to the porphyrin-based COFs.

Zhang et al. (2022a) prepared COF TpPa@rGO composites and used them as cathode for electric sorption of Pb(II) ions from complex solutions. The rGO had the electrical conductivity to provide electrical layers to attract Pb(II) ions, whereas the COF TpPa had enough redox active sites for Pb(II) capture. The rGO and COF TpPa properties resulted in > 99% Pb(II) selective removal from complex solutions with the sorption capacities of 95 mg/g Pb(II) in single solutions and 130 mg/g Pb(II) in multicomponent systems. The complex of COFs with other materials provided promising technique for selective adsorption of metal ions from complex solutions. The modification of special functional groups or porous structure adjust could improve the selective binding of Pb(II) from complex solutions (Ghorbani et al. 2020). Guillem-Navajas et al. (2022) loaded iron oxyhydroxide on COFs to prepare FeOOH@COF composites, which exhibited remarkable sorption efficiency of 98% As(III) in several minutes at pH 5–11. The FeOOH@COF had high selectivity of As(III) removal efficiency rather than other metal ions such as Hg(II) and Pb(II) ions. The imine-lined COFs doped with carbon dots (TaPa-1 COF/CD) composites exhibited high efficiency in the detection and sorption of Hg(II). The composites showed excellent fluorescence detection of Hg(II) and sorption capacity of 235 mg/g (Qin et al. 2022). Folens et al. (2016) prepared Cr-based MOFs for the simultaneous sorption of As(III) and As(V) from aqueous solution, with the sorption capacities of 122 mg/g for As(III) and 80 mg/g As(V). The existence of Mg^{2+}, Ca^{2+}, phosphates and natural organic materials in solution did not affect the removal selectivity and efficiency of As(III) and As(V)

species from wastewater. However, the mechanism of the high selectivity of As(III) and As(V) removal was not discussed in detail. The sorption capacities of different metals by COFs and MOFs nanomaterials, and the comparison with carbon materials are summarized in Table 4. One can see that the sorption capacities of MOFs and COFs nanomaterials were much higher than those of carbon nanomaterials. For the environmental metal pollution treatment, the selective elimination/removal of heavy metal ions from complex wastewater is crucial for the pollutant elimination. The porous structures, the surface functional groups, the active sites and incorporation with other nanomaterials could change and enhance the sorption properties of the nanomaterials.

4.2 Photocatalytic reduction

The in-situ reduction of high valent metal elements to form precipitate is effective to reduce the toxicity and concentration of high valent metal elements (Liu et al. 2023; Wang et al. 2019). Zhong et al. (2020) constructed magnetic COFs (Fe_3O_4/TpPa-1) composites, which showed high sorption capacity of Cr(VI) (245 mg/g) with high reusability and stability. The XPS analysis and materials Studio calculation showed that the imine and carbonyl groups acted as the platform for Cr(VI) binding. The high toxic Cr(VI) could also be reduced to less toxic Cr(III) by the efficient separation and transport of charge carriers. Shi et al. (2022) constructed Ag/AgBr/TzDa COF catalyst and applied it for Cr(VI) photocatalytic reduction and extraction under visible light conditions. The composites showed higher catalytic activity in Cr(VI) reduction than AgBr, TzDa and their mixtures. The photocatalytic reduction of high toxic Cr(VI) to less toxic Cr(III) was mainly attributed to the photogenerated electrons. Yang et al. (2019) constructed CdS/MOFs composites and applied it for Cr(VI) removal. The photocatalytic activity of CdS/MOFs for Cr(VI) reduction was 5 times higher than that of CdS. The CdS/MOFs had higher light absorption and efficient charge transfer/separation ability than CdS and MOFs, thereby exhibited higher photocatalytic activity. The MIL-53(Fe) MOFs catalysts showed excellent photocatalytic ability for Cr(VI) reduction. About 100% Cr(VI) was reduced in 40 min under visible light conditions and also exhibited high reduction ability of Cr(VI) (60% removal) and degradation of dyes (RhB) (80% removal) in 6 h. The iron-oxo cluster adsorbed the incident photons and then the charge carriers transported to MIL-53(Fe) MOFs surface. The synergetic effect of electrons and holes contributed to Cr(VI) reduction and dyes degradation (Liang et al. 2015). Wen et al. (2022) constructed TiO_2@COFs composites and used them for Cr(VI) photocatalytic reduction. The formation of C-O-Ti bond enabled the photoelectrons to transfer from TiO_2 to COFs, and enhanced the separation of photogenerated carriers. The composites also showed high visible light harvest and excellent Cr(VI) reduction. The quenching tests showed that Cr(VI) reduction was suppressed significantly after the addition of $K_2S_2O_8$, whereas the addition of other scavengers did not decrease Cr(VI) reduction obviously (Fig. 3a). The quenching tests indicated that electrons played a major role in Cr(VI) photocatalytic reduction, whereas the other active species such as $O_2^{\bullet-}$, $^{\bullet}OH$ and h^+ did not play important roles in Cr(VI) reduction. From the energy band characterization, the Z-scheme mechanism of Cr(VI) reduction by TiO_2@COFs was proposed (Fig. 3b). The e^-/h^+ pairs were generated under visible light irradiation, and electrons in conduction band (CB) of TiO_2 were transferred to valence band (VB) of COFs, forming build-in field. The high reduction potential of Z-scheme was retained on CB of COFs, and thereby reduced Cr(VI) to Cr(III) by the photoinduced electrons.

Yao et al. (2022b) investigated the extraction of Cr(VI) through photocatalytic reduction strategy under different pH values. After 6 h irradiation, the extraction efficiencies of Cr(VI) from solution increased from 9.1% to 97.5% when the pH decreased from 10 to 4. Cr(VI) was reduced to trivalent Cr(III) with very high selectivity. They firstly used isopropanol as electron donor to photocatalytic extract Cr(VI) from complicated solutions (Yao et al. 2022a). The formation of insoluble polyhydroxy Cr(V) intermediate contributed to the photocatalytic reduction of Cr(VI) and did not form Cr_2O_3 precipitate by adjusting pH values in the existence of competing other metal ions. Through controlling the electric neutrality and inter-molecule reaction, the di-nuclear Cr(V) ($Cr_2(\mu\text{-}O)_2(OH)_4[OCH(CH_3)_2]_2$) complexes were formed as the final products. This method could efficiently extract Cr(VI) from Cr-plating wastewater and stainless steel, and selectively recover Cr(VI) from complicated wastewater (Figs. 3c and d). This technique is also efficient for the success removal of Cr(VI) from real Cr-plating aqueous solution. This work provided a useful method to selectively extract Cr(VI) from wastewater using natural biomaterials through adjusting pH values under visible light conditions. Photocatalytic reduction of the metal ions from high valence to low valence, and the subsequent formation of the precipitates are efficient in decreasing the immobilization of metals in environment, reducing the toxicity of the metals and separating the target metals from complex systems.

5 Radionuclide pollution treatment

Nuclear energy is a distinguished energy and is considered efficient in solving energy crisis. The enrichment of ^{235}U from salt lakes, ocean and radioactive wastewater

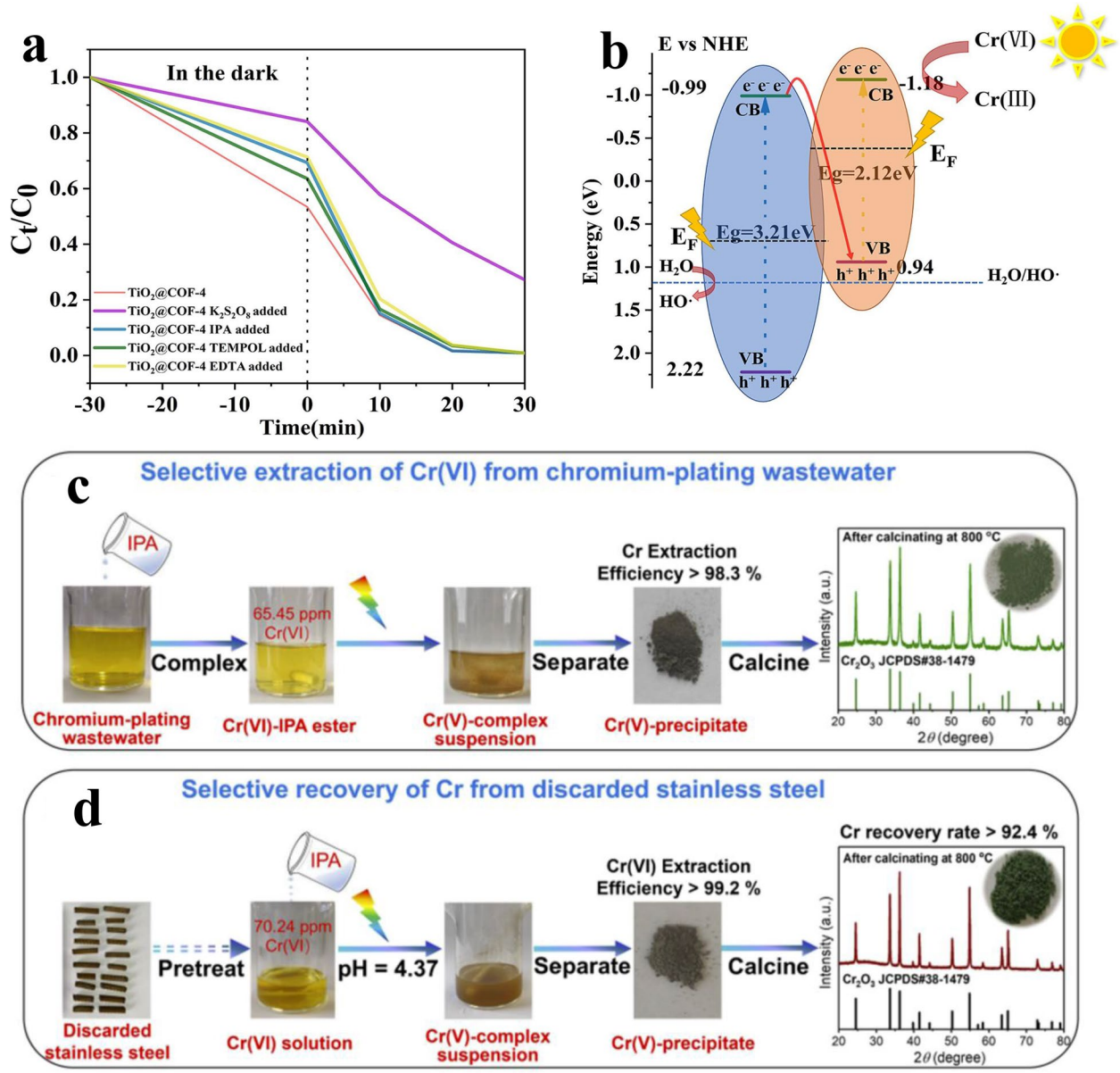

Fig. 3 Photocatalytic reduction of Cr(VI) by TiO_2@COFs by the addition of different scavengers under visible light conditions (**a**) and proposed mechanism of Cr(VI) reduction (**b**) (Wen et al. 2022); The elimination of Cr(VI) by photocatalytic precipitation from real Cr-plating wastewater (**c**) and from discarded stainless steel (**d**) (Yao et al. 2022a)

is important for the continuous development of nuclear energy peaceful utilization (Cai et al. 2023). However, radionuclides are inevitably released into environment during the whole development of nuclear energy. The release of radioactive gases such as ^{85}Kr, ^{127}Xe, $^{129}I_2$ vapor into the atmosphere, the release of $^{235}U(VI)$, $^{99}TcO_4^-$ and other actinides in mining process or spent fuel treatment. The radiotoxicity of radionuclides, especially their irradiation in human body, is much higher than nonradioactive metal ions even though their concentration is 1000 times lower than metal ions. Thereby, the elimination of radionuclides is significant for environment protection and public human safety.

5.1 Sorption

Di et al. (2022) reviewed the removal of $^{99}TcO_4^-$ by COFs as adsorbents from solutions, and found that COFs were suitable materials for $^{99}TcO_4^-$ removal from aqueous solutions with high stability and selectivity. Hao et al. (2022a) synthesized ionic COFs, which had high

Brunner-Emmet-Teller (BET) surface area (> 2700 m^2/g), ordered porous structures, high radiation and chemical stability. The ionic COFs exhibited high selectivity for ReO_4^- and $^{99}TcO_4^-$ sorption in high other anions' concentrations, with the sorption capacity of 1262 mg/g for ReO_4^-. The density functional theory (DFT) calculations further evidenced the strong binding of ReO_4^- and $^{99}TcO_4^-$ on the COFs, suggesting the selective sorption over other anions. The single-exchange COFs modified with alkyl groups were applied to remove $^{99}TcO_4^-$ from aqueous solutions. They found that the COFs exhibited high selectivity and sorption ability, which was attributed to hydrophobicity reaction and steric effect (Li et al. 2021a). Cheng et al. (2021) synthesized amidoxime-modified COFs and used them as adsorbent for the extraction of U(VI) from wastewater and seawater. The prepared COFs exhibited high selectivity and efficiency of U(VI) sorption, with the sorption capacity of 5.1 mg/g from ocean water, 1.6 times higher than V(V) from natural seawater. The DFT calculation further revealed that the binding energy between COFs and U(VI) was much higher than those of V(V), and the bond distances of U(VI) with COFs were shorter than that of V(V) with COFs. The theoretical simulation results indicated the higher selectivity of U(VI) than V(V) in seawater. Yang et al. (2017) constructed GO-COOH/UiO-66 MOFs composites for U(VI) separation from simulated seawater, and found that the composites achieved the sorption capacity of 188 mg/g, which was attributed to the sorption sites of GO-COOH sheets. The XPS and FTIR analysis indicated that the ion exchange and chelation occurred on the GO-COOH nanosheets, thereby increased the sorption ability and selectivity. The separation of U(VI)/Ln(III) by Fe_3O_4@ZIF-8 MOFs composites showed ultrahigh sorption capacity of U(VI) (523 mg/g) with remarkable selectivity of U(VI) from lanthanides containing solutions. The spectroscopy analysis and theoretical calculation showed that H-bonding together with the coordination of Zn centers and U(VI) ions contributed to the high U(VI) uptake (Min et al. 2017). Liu et al. (2022c) synthesized Cu_xPc-COFs composites using microwave irradiation technique. The prepared Cu_xPc-COFs had high iodine capture ability with 492 mg/g iodine from cyclohexane solution and 2.99 g/g iodine vapor. The DFT calculation showed high sorption if iodine was related to the charge transfer and π-conjugated structures of Cu_xPc-COFs with iodine molecules. The selective removal of radionuclides from wastewater is mainly dependent on the strong complexes ability of the surface functional groups with the target radionuclide. The porous structures and inner channels also contribute to the selective binding of the target radionuclides. COFs nanomaterials with designed structures, active sites and special functional groups could achieve the selective extraction of radionuclides from solutions.

5.2 Photocatalytic reduction

Photocatalytic reduction of U(VI) is one efficient technique for U(VI) extraction from wastewater or ocean (Chen et al. 2022b; Hu et al. 2023a). Li et al. (2021b) found that U(VI) could be photocatalytically extracted from solution without using catalyst under visible light conditions. In the existence of organics such as alcohol, U(VI) could form unstable U(V), which was further transformed to U(IV) precipitates through disproportionation reactions at optimal pH conditions. This work provided a facile method to extract U(VI) selectively from complex solutions under solar irradiation. Hao et al. (2022b) synthesized the Pd-doped COFs (Fig. 4a) for the selective extraction of U(VI) from seawater through sorption-photoreduction processes (Fig. 4b). U(VI) could be efficiently removed from solution to COFs by the photocatalytic reduction process under visible light conditions (Fig. 4c). The further X-ray absorption fluorescence structure spectroscopy (XAFS) analysis showed that the U(VI) presented as hexavalent U(VI) species on COFs under dark conditions but existed as UO_2 species on COFs under visible light conditions (Fig. 4d), suggesting the photoreduction of UO_2^{2+} to UO_2(s) under natural sunlight irradiation. The amidoxime groups of COFs could bind the U(VI) ions with high selectivity, whereas the bipyridine-Pd and triazine sites could photocatalytically reduce U(VI) to UO_2 solid. The synthesized COFs exhibited U(VI) extraction ability of 4.62 mg/(g·day) U(VI) from natural ocean water. More importantly, the COFs could generate $^*O_2^-$ and $^1O_2$ active free radicals, which not only reduced U(VI) to U(IV), but also had antibiofouling activity, which was very important for sustainable extraction of U(VI) from natural seawater.

5.3 Electrocatalysis

Besides the photocatalytic extraction of U(VI) from seawater, Yang et al. (2021) for the first time applied sorption-electrocatalytic method to extract U(VI) selectively from natural seawater and wastewater. They functionalized porous carbon with FeNx single atoms and amidoxime functional groups. The FeNx porous carbon electrode achieved the U(VI) sorption capacity of ~ 128 mg/g with the removal ratio of 99% in 24 h from 10 ppm U(VI)-spiked seawater (Fig. 5a). The amidoxime group could selectively bind U(VI) ions and the FeNx centres could reduce the adsorbed U(VI) to unstable U(V), and then the unstable U(V) was re-oxidized to form $Na_2O(UO_3{\cdot}H_2O)_x$ solid on the electrode in the presence of Na^+ ions, which was easily to be separated from solutions. This method could extract

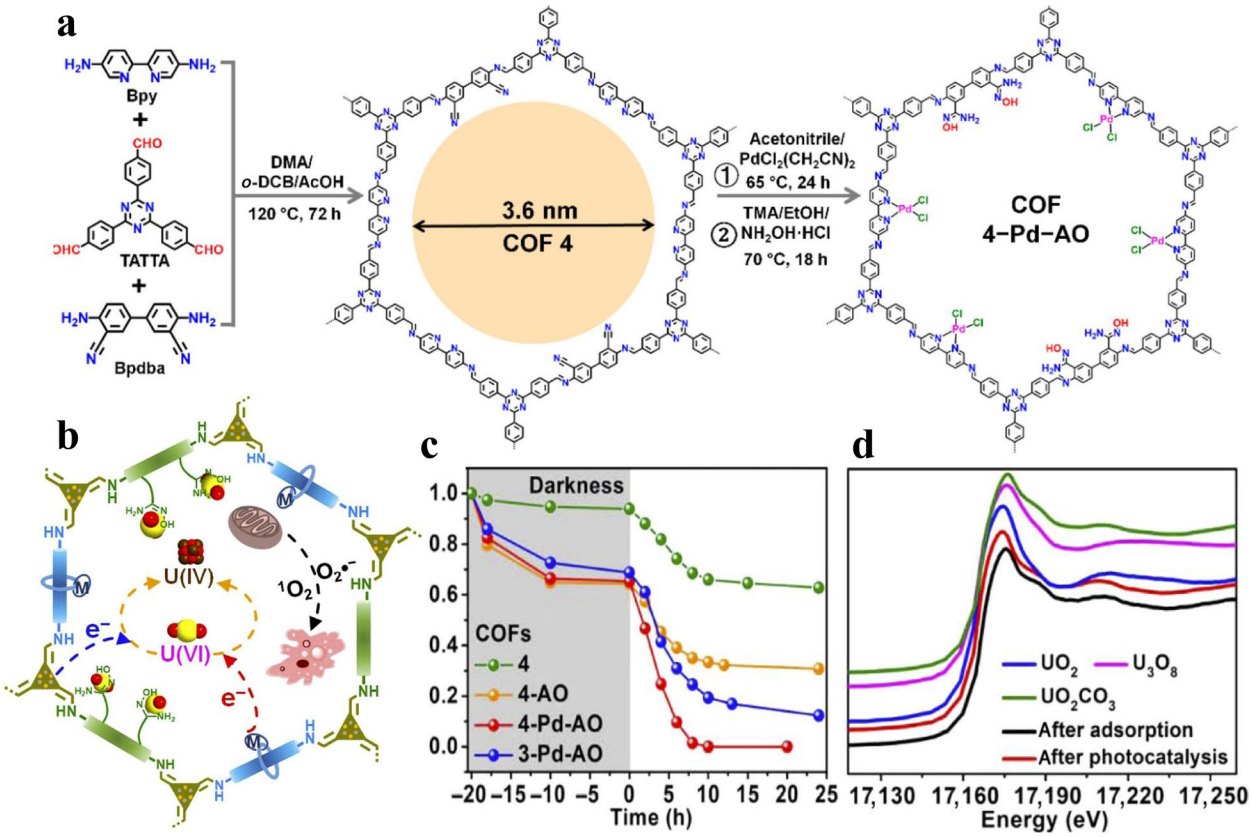

Fig. 4 The synthesis of COF material (**a**); Sorption-photocatalytic extraction strategy for U(VI) extraction from solutions (**b**); The sorption-photocatalytic reduction of U(VI) from solutions using different COFs (**c**); The XAFS analysis of U(VI) adsorption and U(VI) photocatalytic extraction samples (**d**) (Hao et al. 2022b)

1.2 mg/(g·day) U(VI) from natural seawater, which was the highest value for U(VI) extraction from ocean water. The authors used advanced spectroscopy such as XAFS to measure the structures and coordination of U(VI) on the porous carbon, and the XAFS showed that U(VI) formed U(VI) solid phases on the electrode (Fig. 5b). From the characterization of the precipitates on the electrode, the electrocatalytic extraction mechanism of U(VI) from seawater was described in Fig. 5c. Figure 5d gave the photographs of the FeNx porous carbon electrode in U(VI) electrocatalytic extraction from U(VI)-spiked seawater. One can see that U(VI) was continuously deposited on the electrode in the electrocatalysis processes. However, the formation of UO_2^+ species was not evident directly. They further doped InNx single atoms on porous carbon and functionalized with amidoxime groups to prepare In-Nx-C-R electrocatalyst, and used them to extract U(VI) from ocean water. The formation of unstable UO_2^+ was measured by in-situ Raman spectroscopy (Fig. 5e). The appearance of UO_2^+ signal (810 cm^{-1}) indicated the adsorption and reduction of U(VI) to unstable UO_2^+ intermediates (Pointurier and Marie 2013; Stefaniak et al. 2008). The U(VI) signal intensity decreased with the increase of time and at last disappeared completely, suggesting that the adsorbed U(VI) was completely reduced to UO_2^+ intermediates. It is very interesting to note that a new peak at 374 cm^{-1} was observed, which was attributed to the oxidation of unstable UO_2^+ to stable U(VI) in NaCl solutions. The XAFS analysis further supported the appearance of $Na_2O(UO_3{\cdot}H_2O)_x$ solid on the In-Nx-C-R electrode (Liu et al. 2022d). The authors pointed out that $Na_2O(UO_3{\cdot}H_2O)_x$ was formed only in the presence of Na^+ ions, and it was a general method to precipitate U(VI) on the electrode. The electrocatalytic extraction strategy is important for the selective removal of U(VI) ions continuously from seawater or complex solutions. In the electrocatalytic extraction process, it is not necessary to consider the experimental conditions such as visible light utilization, coexisted cations. More importantly, the radionuclides could be extracted from solutions and formed precipitates on the electrode continuously.

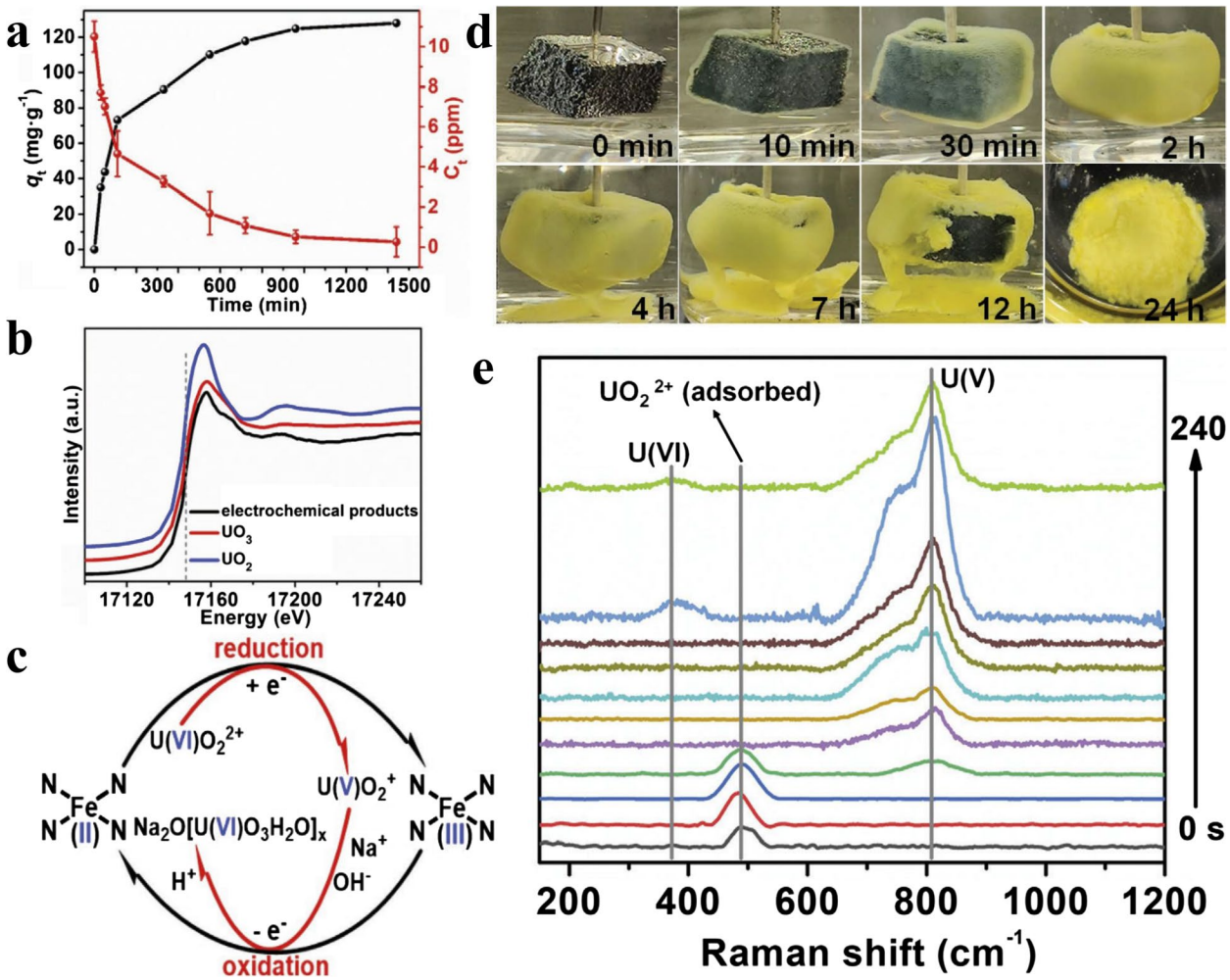

Fig. 5 Electrocatalytic strategy for the extraction of U(VI) from 10 ppm U(VI)-spiked seawater (**a**); The XAFS spectra for electrochemically products using Fe–Nx–C–R as catalyst (**b**); Plausible reaction mechanism for U(VI) extraction from seawater using Fe–Nx–C–R as catalyst (**c**); Photographs of Fe–Nx–C–R electrode in U(VI)-spiked seawater ($C[U(VI)]_{initial} = 1000$ ppm) using electrocatalytic extraction (**d**); In-situ Raman spectra collected from In — Nx — C — R electrode in U(VI)-spiked seawater in adsorption — electrocatalysis processes (**e**). (Liu et al. 2022d; Yang et al. 2021)

5.4 Piezocatalysis

Besides photocatalysis and electrocatalysis extraction of radionuclides, peizocatalytic extraction of radionuclides is a new promising technique. The external mechanical vibration causes the change of surface charge density. Under mechanical stretches and stresses condition, the negative and positive charges move in the material due to the piezoelectric effect and thereby result in piezo properties (Li et al. 2023). Cai et al. (2022) found that piezocatalytic materials could generate the active free radicals such as *OH, $*O_2^-$ and $^1O_2$ under ultrasonic conditions, which could reduce U(VI) to form UO_2(s) by the piezo-generated free radicals. More importantly, H_2O_2 was also generated in the piezocatalytic processes, which further re-oxidized UO_2 to $(UO_2)O_2{\cdot}2H_2O$, and thereby formed precipitates on the piezocatalyst. This method provided an efficient technique to selectively separate U(VI) from complex wastewater. Gao et al. (2022) investigated the piezo-catalytic extraction of Cr(VI) ions from wastewater and found that Cr(VI) was piezo-catalytic reduced to Cr(III) under ultrasonic conditions on its surface. The generated electrons-holes, *OH and H_2O_2 contributed to the piezo-catalytic reduction of Cr(VI) from toxic hexavalent to less toxic trivalent. To enhance the piezocatalytic ability, the defect introduction of the piezocatalyst is the efficient method. The metal-doping, introduction of interface or intrinsic defects and heterogeneous metal oxides-loading could enhance the piezo-generation and e^-/h^+ separation, and the generation of active free species under ultrasonic conditions. Till now, the

piezo-reduction of high valent metal elements to its low valent elements using MOFs or COFs still has not been extensively studied. The MOFs or COFs with piezocatalytic properties, tunable porous structures and active sites could be promising piezocatalytic materials in efficient piezocatalytic extraction of radionuclides and metals selectively from complicated solutions. With the development of technology, the piezo-catalysis strategy for the environmental pollution cleanup will attract more and more interest in the future.

6 Conclusions and perspectives

In this paper, we summarized the application of MOFs and COFs nanomaterials for the elimination of organic contaminants, radionuclides and metal ions through sorption and catalysis (photocatalysis, electrocatalysis, piezocatalysis) processes. Different kinds of techniques for the removal of the (in)organic pollutants have been studied extensively, herein the sorption and catalysis strategies for the decontamination of pollutants by MOFs and COFs nanomaterials were reviewed. The sorption and photocatalytic degradation of organic contaminants were the efficient technique for organic contaminants elimination from aqueous solutions. The advantages of COFs and MOFs nanomaterials in the elimination of pollutants can be summarized as: 1) the sorption capacities of MOFs and COFs are much higher than those of today's most reported materials because of their high surface areas, abundant functional groups and active sites; 2) the COFs or MOFs nanomaterials have the high efficiency in the removal of (in)organic contaminants from complex systems; 3) the modification of special functional groups or tunable porous structure, the target pollutants could be eliminated selectively; 4) the catalytic reduction/extraction could selectively extract metal ions from complex wastewater; 5) the COFs and MOFs nanomaterials have high reusability and stability, especially under extreme conditions, which is crucial for real applications; and 6) to enhance the elimination efficiency, the doping of single metal atoms or metal oxides, or the incorporation with other nanomaterials to change the porosity, the porous structure, active sites and functional groups are helpful for improving the sorption ability or catalytic capacity.

Although the MOFs and COFs nanomaterials have super abilities in environmental pollution treatment, there are still some difficulties for the real applications such as: 1) the MOFs or COFs cannot be synthesized in large scale at low cost now. At current stage, the materials are easily synthesized in laboratory level, but still difficult to be industrially synthesized; 2) the separation of the materials from solutions is still difficult if the nanomaterial powders are used in wastewater treatment. The incorporation of the nanomaterials with other materials for easy separation is the useful technique; 3) the toxicity of the released nanomaterials should be considered. The nanomaterial toxicity to ecosystem is the inevitable problem for the low contents of nanomaterials in environment; 4) the high efficient removal of target pollutant is still difficult. The surface grafting technique is very important method to realize the selective binding of target pollutant by different functional groups. However, the high selective elimination of pollutant from complex systems is still a problem; 5) the enhancement of visible light absorption, the e^-/h^+ generation and separation are the main challenges in photocatalysis. For the efficient removal of contaminants by photocatalysis strategy, the improvement of the photocatalytic activity is the best method to increase the pollutant removal efficiency; 6) the price of COFs and MOFs is still much higher than that of traditional materials such as active carbon. The high removal ability and reusability could partly reduce the cost for real applications. With the development of technology, such nanomaterials may be industrially synthesized, which could reduce the price of MOFs and COFs significantly. From the physicochemical properties, one can see that the MOFs, COFs and MOFs/COFs-based nanomaterials will be applied in large scale in real applications in pollution treatment.

Abbreviations

4-CP	4-Chlorophenol
BET	Brunner — Emmet — Teller
BH	Berberine hydrochloride
BPA	Bisphenol A
CB	Conduction band
COFs	Covalent organic frameworks
COP-NH_2	Covalent organic polymer modified with tetrathylenepentamine
CR	Congo red
DFT	Density functional theory
DMPO	5,5-Dimethyl-1-pyrroline
EBT	Eriochrome black T
EBR	Eriochrome blue R
ESR	Electron spin resonance
MB	Methylene blue
MO	Methyl orange
MOFs	Metal organic frameworks
nZVI	Nano-zero valent iron
PAHs	Polycyclic aromatic hydrocarbons
POPs	Persistent organic pollutants
PFOS	Perfluorooctane sulfonate
rGO	Reduced graphene
ROSs	Reactive oxygen species
RhB	Rhodamine B
TEMP	2,2,6,6-Tetramethyl-4-piperidinol
TEMPO	2,2,6,6-Tetramethylpiperidine 1-oxyl
TpPa@rGO	COF-reduced graphene
VB	Valence band
XAFS	X-ray absorption fluorescence structure

Acknowledgements
The authors acknowledged the anonymous reviewers for favorable comments to improve the quality of this review.

Authors' contributions
Zhongshan Chen: investigation, writing original draft; Yang Li: investigation and review; Yawen Cai: Investigation and review; Suhua Wang: review & editing; Baowei Hu: investigation, review & editing; Bingfeng Li: review and investigation; Xiaodong Ding: investigation; Li Zhuang: review and investigation; Xiangke Wang: writing, review & editing. The author(s) read and approved the final manuscript.

Funding
National Natural Science Foundation of China (22276054), National Key Research and Development Program of China (2018YFC1900105) and Beijing Outstanding Young Scientist Program.

Availability of data and materials
Authors can confirm that all relevant data are included in the article.

Declarations

Ethical approval and consent to participate
No.

Consent for publication
Agree.

Competing interests
Xiangke Wang is an editorial board member for Carbon Research and was not involved in the editorial review, or the decision to publish, this article. All authors declare that there are no competing interests.

Author details
[1]College of Environmental Science and Engineering, North China Electric Power University, Beijing 102206, P.R. China. [2]School of Life Science, Shaoxing University, Shaoxing 312000, P.R. China. [3]School of Environmental Science and Engineering, Guangdong University of Petrochemical Technology, Maoming 525000, P.R. China. [4]Power China Sichuan Electric Power Engineering Co., Ltd, Chengdu 610041, P.R. China. [5]Zhejiang Jinjiang Environment Holding Company Limited, Hangzhou 310011, P.R. China.

Received: 28 November 2022 Revised: 25 January 2023 Accepted: 28 January 2023
Published online: 09 February 2023

References

Ahmed MB, Zhou JL, Ngo HH, Guo WS (2015) Adsorptive removal of antibiotics from water and wastewater: progress and challenges. Sci Total Environ 532:112–126
Ahmed MB, Zhou JL, Ngo HH, Guo W, Chen MF (2016) Progress in the preparation and application of modified biochar for improved contaminant removal from water and wastewater. Bioresource Technol 214:836–851
Amin M, Chetpattananondh P (2019) Biochar from extracted marine Chlorella sp. residue for high efficiency adsorption with ultrasonication to remove Cr(VI), Zn(II) and Ni(II). Bioresource Technol 289:121578
Barea E, Montoro C, Navvrro JAR (2014) Toxic gas removal – metal-organic frameworks for the capture and degradation of toxic gases and vapours. Chem Soc Rev 43:5419–5430
Biswal BP, Chandra S, Kandambeth S, Lukose B, Heine T, Banerjee R (2013) Mechanochemical synthesis of chemically stable isoreticular covalent organic frameworks. J Am Chem Soc 135:5328–5331
Cai Y, Zhang Y, Lv Z, Zhang S, Gao F, Fang M, Kong M, Liu P, Tan X, Hu B, Wang X (2022) Highly efficient uranium extraction by a piezo catalytic reduction-oxidation process. Appl Catal B: Environ 310:121343
Cai Y, Fang M, Hu B, Wang X (2023) Efficient Extraction of Uranium Ions from Solutions. Nucl Sci Technol 34:2
Canivet J, Fateeva A, Guo Y, Coasne B, Farrusseng D (2014) Water adsorption in MOFs: fundamentals and applications. Chem Soc Rev 43:5594–5617
Cao M, Lei J, Zhang J, Zhou L, Liu Y (2022) Covalent organic frameworks derived carbon supported cobalt ultra-small particles: C═O and Co-Nx complex sites activated peroxymonosulfate synergistically for efficient degradation of levofloxacin. J Clean Prod 375:134114
Chen W, Yang Z, Xie Z, Li Y, Yu X, Lu F, Chen L (2019) Benzothiadiazole functionalized D-A type covalent organic frameworks for effective photocatalytic reduction of aqueous chromium(VI). J Mater Chem A 7:998–1004
Chen H, Gao Y, Li J, Fang Z, Bolan N, Bhatnagar A, Gao B, Hou D, Wang S, Song H, Yang X, Shaheen SM, Meng J, Chen W, Rinklebe J, Wang H (2022a) Engineered biochar for environmental decontamination in aquatic and soil systems: a review. Carbon Res 1:4
Chen T, Yu K, Dong C, Yuan X, Gong X, Lian J, Cao X, Li M, Zhou L, Hu B, He R, Zhu W, Wang X (2022b) Advanced photocatalysts for uranium extraction: Elaborate design and future perspectives. Coord Chem Rev 467:214615
Chen ZS, He X, Li Q, Yang H, Liu Y, Wu LN, Liu ZX, Hu BW, Wang XK (2022c) Low-temperature plasma induced phosphate groups onto coffee residue-derived porous carbon for efficient U(VI) extraction. J Environ Sci 122:1–13
Cheng G, Zhang A, Zhao Z, Chai Z, Hu B, Han B, Ai Y, Wang X (2021) Extremely stable amidoxime functionalized covalent organic frameworks for uranium extraction from seawater with high efficiency and selectivity. Sci Bull 66:1994–2001
Cote AP, Benin AI, Ockwig NW, O'Keeffe M, Matzger AJ, Yaghi OM (2005) Porous, crystalline, covalent organic frameworks. Science 310:1166–1170
Czaja AU, Trukhan N, Muller U (2009) Industrial applications of metal-organic frameworks. Chem Soc Rev 38:1284–1293
Di ZY, Moa YN, Yuan H, Zhou Y, Jin J, Li CP (2022) Covalent organic frameworks (COFs) for sequestration of $^{99}TcO_4^-$. Chem Res Chin Univ 38:290–295
Ding SY, Wang W (2013) Covalent organic frameworks (COFs): from design to applications. Chem Soc Rev 42:548–568
Ding SY, Dong M, Wang YW, Chen YT, Wang HZ, Su CY, Wang W (2016) Thioether-based fluorescent covalent organic framework for selective detection and facile removal of mercury(II). J Am Chem Soc 138:3031–3037
Dong L, Li S, Jin Y, Hu B, Sheng G (2021) Enhanced adsorption of Eu(III) from wastewater using *Solidago canadensis*-derived biochar functionalized by Ca/Al-LDH and hydroxyapatite. Appl Surf Sci 567:150794
Feng X, Ding X, Jiang DL (2012) Covalent organic frameworks. Chem Soc Rev 41:6010–6022
Folens K, Leus K, Nicomel NR, Meledina M, Turner S, Tendeloo GV, Laing GD, Voort PVD (2016) Fe_3O_4@MIL-101 – A selective and regenerable adsorbent for the removal of As species from water. Eur J Inorg Chem 27:4395–4401
Gao FX, Fang M, Zhang S, Ni MY, Cai YW, Zhang YF, Tan XL, Kong MG, Xu W, Wang XK (2022) Symmetry-breaking induced piezocatalysis of Bi_2S_3 nanorods and boosted by alternating magnetic field. Appl Catal B: Environ 316:121664
Ghorbani M, Seyedin O, Ahamohammadhassan M (2020) Adsorptive removal of lead(II) ion from water and wastewater media using carbon-based nanomaterials as unique sorbents: a review. J Environ Manage 254:109814
Gong W, Cui H, Xie Y, Li Y, Tang X, Liu Y, Cui Y, Chen B (2021) Efficient C_2H_2/CO_2 separation in ultramicroporous metal—organic frameworks with record C_2H_2 storage density. J Am Chem Soc 143:14869–14876
Gu H, Liu X, Wang S, Chen Z, Yang H, Hu B, Shen C, Wang X (2022) COF-based composites: extraordinary removal performance for heavy metals and radionuclides from aqueous solutions. Rev Environ Contam Toxicol 260:23
Guillem-Navajas A, Martin-Illan JA, Salagre E, Michel EG, Rodriguez-San-Miguel D, Zamora F (2022) Iron oxyhydroxide-covalent organic framework nanocomposites for efficient As(III) removal in water. ACS Appl Mater Interface 14:50163–50170
Guo Z, Jiang H, Wu H, Zhang L, Song S, Chen Y, Zheng C, Ren Y, Zhao R, Li Y (2021) Oil-water-oil triphase synthesis of ionic covalent organic framework nanosheets. Angew Chem Int Ed 60:27078–27085

Gupta VK, Saleh TA (2013) Sorption of pollutants by porous carbon, carbon nanotubes and fullerene - an overview. Environ Sci Pollut Res 20:2828–2843

Hao M, Chen Z, Yang H, Waterhouse GIN, Ma S, Wang X (2022a) Pyridinium salt-based covalent organic framework with well-defined nanochannels for efficient and selective capture of aqueous $^{99}TcO_4^-$. Sci Bull 67:924–932

Hao M, Chen Z, Liu X, Liu X, Zhang J, Yang H, Waterhouse GIN, Wang X, Ma S (2022b) Converging cooperative functions into the nanospace of covalent organic frameworks for efficient uranium extraction from seawater. CCS Chem 4:2294–2307

Hao M, Xie Y, Liu X, Chen Z, Yang H, Waterhouse GIN, Ma S, Wang X (2023) Modulating the uranium extraction performance of multivariate covalent organic frameworks through donor—acceptor linkers and amidoxime nanotraps. JACS Au. 3: 239-251

He L, Chen L, Dong X, Zhang S, Zhang M, Dai X, Liu X, Lin P, Li K, Chen C, Pan T, Ma F, Chen J, Yuan M, Zhang Y, Chen L, Zhou R, Han Y, Chai Z, Wang S (2021) A nitrogen-rich covalent organic framework for simultaneous dynamic capture of iodine and methyl iodide. Chem 7:699–714

Hu Y, Tang D, Shen Z, Yao L, Zhao G, Wang X (2023a) Photochemically triggered self-extraction of uranium from aqueous solution under ambient conditions. Appl Catal B: Environ 322:122092

Hu Y, Wang S, Zhang L (2023b) Yang F (2023b) Selective removal of Hg(II) by UiO-66-NH_2 modified by 4-quinolinecarboxaldehyde: from experiment to mechanism. Environ Sci Pollut Res 30:2283–2297

Huang N, Zhai LP, Xu H, Jiang DL (2017) Stable covalent organic frameworks for exceptional mercury removal from aqueous solutions. J Am Chem Soc 139:2428–2434

Huang LJ, He M, Chen BB, Hu B (2018) Magnetic Zr-MOFs nanocomposites for rapid removal of heavy metal ions and dyes from water. Chemosphere 199:435–444

Huang D, Liu C, Zhang C, Deng R, Wang R, Xue W, Luo H, Zeng G, Zhang Q, Guo X (2019) Cr(VI) removal from aqueous solution using biochar modified with Mg/Al-layered double hydroxide intercalated with ethylenediaminetetraacetic acid. Bioresource Technol 276:127–132

Huang LTY, Cao H, Ma JZ, Wang XX (2022) Efficient removal of Pb(II) by UiO-66-NH_2: a combined experimental and spectroscopic studies. Environ Nanotechnol Monit Manage 18:100741

Hussain M, Maile N, Tahir K, Ghani AA, Kim B, Jang J, Lee DS (2022) Flexible thiourea-based covalent organic frameworks for ultrahigh mercury removal from aqueous solutions. Chem Eng J 446:137410

Jin WL, Ji X, Hou XL, Ji SY, Li W, Yu X, Liu XW, Zhu LN, Jiang HX, Kong DM (2022) Porphyrin COF and its mechanical pressing-prepared carbon fiber hybrid membrane for ratiometric detection, removal and enrichment of Cd^{2+}. J Hazard Mater 439:129574

Kang K, Li L, Zhang M, Zhang X, Lei L, Xiao C (2021) Constructing cationic metal—organic framework materials based on pyrimidyl as a functional group for perrhenate/pertechnetate sorption. Inorg Chem 60:16420–16428

Karak S, Kandambeth S, Biswal B, Sasmal H, Kumar S, Pachfule P, Banerjee R (2017) Constructing ultraporous covalent organic frameworks in seconds via an organic terracotta process. J Am Chem Soc 139:1856–1862

Kitagawa SJ (2014) Metal–organic frameworks (MOFs). Chem Soc Rev 43:5415–5418

Kong K, Cheng B, Liang J, Guo Y, Wang R (2022) The aminated covalent organic polymers for reversible removal of concurrent perfluorooctane sulfonate and dichromate. Chem Eng J 446:137343

Li JR, Kuppler RJ, Zhou HC (2009) Selective gas adsorption and separation in metal-organic frameworks. Chem Soc Rev 38:1477–1504

Li C, Zhang L, Gao Y, Li A (2018a) Facile synthesis of nano ZnO/ZnS modified biochar by directly pyrolyzing of zinc contaminated corn stover for Pb(II), Cu(II) and Cr(VI) removals. Waste Manage 79:625–637

Li J, Wang X, Zhao G, Chen C, Chai Z, Alsaedi A, Hayat T, Wang X (2018b) Metal–organic framework-based materials: superior adsorbents for the capture of toxic and radioactive metal ions. Chem Soc Rev 47:2322–2356

Li Y, Zhang H, Chen Y, Huang L, Lin Z, Cai Z (2019) Core—shell structured magnetic covalent organic framework nanocomposites for triclosan and triclocarban adsorption. ACS Appl Mater Interfaces 11:22492–22500

Li Z, Meng Q, Yang Y, Zou X, Yuan Y, Zhu G (2020) Constructing amidoxime-modified porous adsorbents with open architecture for cost effective and efficient uranium extraction. Chem Sci 11:4747

Li J, Li B, Shen N, Chen L, Guo Q, Chen L, He L, Dai X, Chai Z, Wang S (2021a) Task-specific tailored cationic polymeric network with high base-resistance for unprecedented $^{99}TcO_4^-$ cleanup from alkaline nuclear waste. ACS Cent Sci 7:1441–1450

Li S, Hu Y, Shen Z, Cai Y, Ji Z, Tan X, Liu Z, Zhao G, Hu S, Wang X (2021b) Rapid and selective uranium extraction from aqueous solution under visible light in the absence of solid photocatalyst. Sci China Chem 64:1323–1331

Li W, Hu Z, Meng J, Zhang X, Gao W, Chen M, Wang J (2021c) Zn-based metal organic framework-covalent organic framework composites for trace lead extraction and fluorescence detection of TNP. J Hazard Mater 411:125021

Li C, Guggenberger P, Han SW, Ding WL, Kelitz F (2022a) Ultrathin covalent organic framework anchored on graphene for enhance organic pollutant removal. Angew Chem Int Ed 61:e202206564

Li K, Luan TX, Wang ZY, Wang JR, Li PZ (2022b) Synergistic effect of functionalization and crystallinity in nanoporous organic frameworks for effective removal of metal ions from aqueous solution. ACS Appl Nano Mater 5:15228–15236

Li Y, Shaheen S, Azeem M, Zhang L, Feng C, Peng J, Qi W, Liu J, Luo Y, Peng Y, Ali E, Smith K, Rinklebe J, Zhang Z, Li R (2022c) Removal of lead (Pb^{+2}) from contaminated water using a novel MoO_3-biochar composite: Performance and mechanism. Environ Poll 308:119693

Li JL, Liu XL, Zhao GX, Liu ZX, Cai YW, Wang SH, Shen C, Hu BW, Wang XK (2023) Piezoelectric materials and techniques for environmental pollution remediation. Sci Total Environ 869:161767

Liang R, Jing F, Shen L, Qin N, Wu L (2015) MIL-53(Fe) as a highly efficient bifunctional photocatalyst for the simultaneous reduction of Cr(VI) and oxidation of dyes. J Hazard Mater 287:364–372

Liu XL, Ma R, Zhuang L, Hu BW, Chen JR, Liu XY, Wang XK (2021a) Recent developments of doped g-C_3N_4 photocatalysts for the degradation of organic pollutants. Cri Rev Environ Sci Technol 51:751–790

Liu XL, Pang HW, Liu XW, Li Q, Zhang N, Mao L, Qiu MQ, Hu BW, Yang H, Wang XK (2021b) Orderly porous covalent organic frameworks-based materials: superior adsorbents for pollutants removal from aqueous solutions. The Innovation 2:100076

Liu G, Dai Z, Liu X, Dahlgren RA, Xu J (2022a) Modification of agricultural wastes to improve sorption capacities for pollutant removal water – a review. Carbon Res 1:24

Liu X, Verma G, Chen Z, Hu B, Huang Q, Yang H, Ma S, Wang X (2022b) Metal-organic framework nanocrystals derived hollow porous materials: synthetic strategies and emerging applications. The Innovation 3:100281

Liu X, Zhang A, Ma R, Wu B, Wen T, Ai Y, Sun M, Jin J, Wang S, Wang X (2022c) Experimental and theoretical insights into copper phthalocyanine-based covalent organic frameworks for highly efficient radioactive iodine capture. Chinese Chem Lett 33:3549–3555

Liu X, Xie Y, Hao M, Chen Z, Yang H, Waterhouse GIN, Ma S, Wang X (2022d) Highly efficient electrocatalytic uranium extraction from seawater over an amidoxime—functionalized In—N—C catalyst. Adv Sci 9:2201735

Liu Z, Xu Z, Buyong F, Chay TC, Li Z, Cai Y, Hu B, Zhu Y, Wang X (2022e) Modified biochar: synthesis and mechanism for removal of environmental heavy metals. Carbon Res 1:8

Liu F, Lou Y, Xia F, Hu B (2023) Immobilizing nZVI particles on MBenes to enhance the removal of U(VI) and Cr(VI) by adsorption-reduction synergistic effect. Chem Eng J 454:140318

Lu Y, Cai Y, Zhuang L, Hu B, Wang S, Chen J, Wang X (2022) Application of biochar-based photocatalysts for sorption-(photo)degradation/reduction of environmental contaminants: Mechanism, challenges and perspective. Biochar 4:45

Lyu H, Xia S, Tang J, Zhang Y, Gao B, Shen B (2020) Thiol-modified biochar synthesized by a facile ball-milling method for enhanced sorption of inorganic Hg^{2+} and organic CH_3Hg^+. J Hazard Mater 384:121357

Mahata P, Madras G, Natarajan S (2006) Novel photocatalysts for the decomposition of organic dyes based on metal-organic framework compounds. J Phys Chem B 110:13759–13768

Maschita J, Banerjee T, Savasci G, Haase F, Ochsenfeld C, Lotsch BV (2020) Ionothermal synthesis of imide-linked covalent organic frameworks. Angew Chem Int Ed 59:15750–15758

Mauter MS, Elimelech M (2008) Environmental applications of carbon-based nanomaterials. Environ Sci Technol 42:5843–5859

Min X, Yang W, Hui Y, Gao C, Dang S, Sun Z (2017) Fe_3O_4@ZIF-8: a magnetic nanocomposite for highly efficient UO_2^{2+} adsorption and selective UO_2^{2+}/Ln^{3+} separation. Chem Commun 53:4199–4202

Muslim M, Ali A, Ahmad M, Alarifi A, Afzal M, Sepay N, Dege N (2022) A zinc(II) metal-organic complex based on 2-(2-aminophenyl)-1H-benzimidazole ligand: Exhibiting high adsorption capacity for aromatic hazardous dyes and catecholase mimicking activity. J Mol Liquid 363:119767

Niu F, Tao L, Deng Y, Gao H, Liu J, Song W (2014) A covalent triazine framework as an efficient catalyst for photodegradation of methylene blue under visible light illumination. New J Chem 38:5695–5699

Pointurier F, Marie O (2013) Use of micro-Raman spectrometry coupled with scanning electron microscopy to determine the chemical form of uranium compounds in micrometer-size particles. J Raman Spectroscopy 44:1753–1579

Qin S, He X, Jin F, Wang Y, Chu H, Han S, Sun Y, Gao L (2022) A facile imine-linked covalent organic framework doped with a carbon dot composite for the detection and removal of Hg^{2+} in surface water. RSC Adv 12:18784–18793

Ren S, Bojdys MJ, Dawson R, Laybourn A, Khimyak YZ, Adams DJ, Cooper AI (2012) Porous, fluorescent, covalent triazine-based frameworks via room-temperature and microwave-assisted synthesis. Adv Mater 24:2357–2361

Rouhani F, Morsali A (2018) Goal-directed design of metal–organic frameworks for Hg(II) and Pb(II) adsorption from aqueous solutions. Chem Eur J 24:17170–17179

Shen L, Liang S, Wu W, Liang R, Wu L (2013) Multifunctional NH_2-mediated zirconium metal-organic framework as an efficient visible-light-driven photocatalyst for selective oxidation of alcohols and reduction of aqueous Cr(VI). Dalton Trans 42:13649–13657

Shen N, Yang Z, Liu S, Dai X, Xiao C, Taylor-Pashow K, Li D, Yang C, Li J, Zhang Y, Zhang M, Zhou R, Chai Z, Wang S (2020) $^{99}TcO_4^-$ removal from legacy defense nuclearwaste by an alkaline-stable 2D cationic metal organic framework. Nat Commun 11:5571

Shen H, Chen L, Zhou C, Du J, Lu C, Yang H, Tan L, Zeng X, Dong L (2022) Immobilizing Fe^0 nanoparticles on covalent organic framework towards enhancement of Cr(VI) removal by adsorption and reduction synergistic effect. Sep Purif Technol 290:120883

Shi Z, Chen Z, Zhang Y, Wang X, Lu T, Wang Q, Zhan J, Zhang P (2022) COF TzDa/Ag/AgBr Z-scheme heterojunction photocatalyst for efficient visible light driven elimination of antibiotics tetracycline and heavy metal ions Cr(VI). Sep Purif Technol 288:120717

Stefaniak EA, Alsecz A, Sajó IE, Worobiec A, Máthé Z, Török S, Grieken VR (2008) Recognition of uranium oxides in soil particulate matter by means of μ-Raman spectrometry. J Nucl Mater 381:278–283

Tan XF, Liu YG, Gu YL, Xu Y, Zeng GM, Hu XJ, Liu SB, Wang X, Liu SM, Li J (2016) Biochar-based nano-composites for the decontamination of wastewater: a review. Bioresource Technol 212:318–333

Tchinsa A, Hossain MF, Wang T, Zhou YJC (2021) Removal of organic pollutants from aqueous solution using metal organic frameworks (MOFs)-based adsorbents: A review. Chemosphere 284:131393

Tran HN, Wang YF, You SJ, Chao HP (2017) Insights into the mechanism of cationic dye adsorption on activated charcoal: the importance of π-π interactions. Pro Safety Environ Prot 107:168–180

Tran HN, Tomul F, Ha NTH, Nguyen DT, Lima EC, Le GT, Chang CT, Masindi V, Woo SH (2020) Innovative spherical biochar for pharmaceutical removal from water: insight into adsorption mechanism. J Hazard Mater 394:122255

Tuziuti T, Yasui K, Lee J, Kozuka T, Towata A, Iida Y (2008) Mechanism of enhancement of sonochemical-reaction efficiency by pulsed ultrasound. J Phys Chem A 112:4875–4878

Voorde BV, Bueken B, Denayer J, Vos DD (2014) Adsorptive separation on metal-organic frameworks in the liquid phase. Chem Soc Rev 43:5766–5788

Wang SB, Sun HQ, Ang HM, Tade MO (2013) Adsorption remediation of environmental pollutants using novel graphene-based nanomaterials. Chem Eng J 226:336–347

Wang D, Jia F, Wang H, Chen F, Fang Y, Dong W, Zeng G, Li X, Yang Q, Yuan X (2018) Simultaneously efficient adsorption and photocatalytic degradation of tetracycline by Fe-based MOFs. J Colloid Interface Sci 519:273–284

Wang HH, Guo H, Zhang N, Chen ZS, Hu BW, Wang XK (2019) Enhanced photoreduction of U(VI) on C_3N_4 by Cr(VI) and bisphenol A: ESR, XPS and EXAFS investigation. Environ Sci Technol 53:6454–6461

Wang H, Wang H, Wang Z, Tang L, Zeng G, Xu P, Chen M, Xiong T, Zhou C, Li X, Huang D, Zhu Y, Wang Z, Tang J (2020a) Covalent organic framework photocatalysts: structures and applications. Chem Soc Rev 49:4135–4165

Wang Q, Gao QY, Ai-Enizi AM, Nafady A, Ma SQ (2020b) Recent advances in MOF-based photocatalysis: environmental remediation under visible light. Inorg Chem Front 7:300–339

Wang L, Tao Y, Wang J, Tian M, Liu S, Quan T, Yang L, Wang D, Li X, Gao D (2022a) A novel hydroxyl-riched covalent organic framework as an advanced adsorbent for the adsorption of anionic azo dyes. Anal Chim Acta 1227:340329

Wang S, Shi L, Yu S, Pang H, Qiu M, Song G, Fu D, Hu B, Wang XX (2022b) Effect of shewanella oneidensis MR-1 on U(VI) sequestration by montmorillonite. J Environ Radioact 242:106798

Wang S, Li Y, Liu Q, Wang J, Zhao Y, Cai Y, Li H, Chen Z (2023) Photo-/electro-/piezo-catalytic elimination of environmental pollutants. J Photochem Photobiology A: Chem 437:114435

Wen R, Li Y, Zhang M, Guo X, Li X, Li X, Han J, Hu S, Tan W, Ma L, Li S (2018) Graphene-synergized 2D covalent organic framework for adsorption: a mutual promotion strategy to achieve stabilization and functionalization simultaneously. J Hazard Mater 358:273–285

Wen Y, Huang Z, Zhao M, Zhao L (2022) Enhanced visible-light-driven photocatalytic activity of bi-phase titanium dioxide@covalent organic framework Z-scheme system for photocatalytic removal of Cr(VI). Appl Surf Sci 596:153485

Xiao Y, Ma C, Jin Z, Wang J, He L, Mu X, Song L, Hu Y (2021) Functional covalent organic framework for exceptional Fe^{2+}, Co^{2+} and Ni^{2+} removal: an upcycling strategy to achieve water decontamination and reutilization as smoke suppressant and flame retardant simultaneously. Chem Eng J 421:127837

Xu Z, Tsang DCW (2022) Redox-induced transformation of potentially toxic elements with organic carbon in soil. Carbon Res 1:9

Xu X, Schierz A, Xu N, Cao X (2016) Comparison of the characteristics and mechanisms of Hg(II) sorption by biochars and activated carbon. J Colloid Interf Sci 463:55–60

Xu M, Cai Y, Chen G, Li B, Chen Z, Hu B, Wang X (2022) Efficient selective removal of radionuclides by sorption and catalytic reduction using nanomaterials. Nanomaterials 12:1443

Yaghi OM, Li G, Li H (1995) Selective binding and removal of guests in a microporous metal-organic framework. Nature 378:703–706

Yang P, Liu Q, Liu J, Zhang H, Li Z, Li R, Liu L, Wang J (2017) Interfacial growth of a metal–organic framework (UiO-66) on functionalized graphene oxide (GO) as a suitable seawater adsorbent for extraction of uranium(vi). J Mater Chem A 5:17933–17942

Yang HY, Jiang L, Wang W, Luo ZF, Li J, He ZJ, Yan ZY, Wang JQ (2019) One-pot synthesis of CdS/metal-organic framework aerogel composites for efficient visible photocatalytic reduction of aqueous Cr(VI). RSC Adv 9:37594–37597

Yang H, Liu X, Hao M, Xie Y, Wang X, Tian H, Waterhouse GIN, Kruger PE, Telfer SG, Ma S (2021) Functionalized iron-nitrogen-carbon electrocatalyst provides a reversible electron transfer platform for efficient uranium extraction from seawater. Adv Mater 2021:2106621

Yang H, Liu Y, Chen Z, Waterhouse GIN, Ma S, Wang X (2022) Emerging technologies for uranium extraction from seawater. Sci China Chem 65:2335–2337

Yao L, Hu Y, Zou Y, Ji Z, Hu S, Wang C, Zhang P, Yang H, Shen Z, Tang D, Zhang S, Zhao G, Wang X (2022a) Selective and efficient photo-extraction of aqueous Cr(VI) as solid-state polyhydroxy Cr(V) complex for environment remediation and resources recovery. Environ Sci Technol 56:14030–14037

Yao L, Shen Z, Ji Z, Hu Y, Tang D, Zhao G, Wang X (2022b) Cr(VI) detoxification and simultaneous selective recovery of Cr resource from wastewater via photo-chemical extraction using biomass. Sci Bull 67:924–632

You Z, Zhang N, Guan Q, Xing Y, Bai F, Sun L (2020) High sorption capacity of U(VI) by COF-based material doping hydroxyapatite microspheres: kinetic, equilibrium and mechanism investigation. J Inorg Organomet Polym Mater 30:1966–1979

Yu S, Tang H, Zhang D, Wang SQ, Qiu MQ, Song G, Fu D, Hu BW, Wang XK (2022) MXenes as emerging nanomaterials in water purification and environmental remediation. Sci Total Environ 811:152280
Yuan S, Li X, Zhu J, Zhang G, Puyvelde PV, Bruggen BV (2019) Covalent organic frameworks for membrane separation. Chem Soc Rev 48:2665–2681
Zahed MA, Salehi S, Madadi R, Hejabi F (2021) Biochar as a sustainable product for remediation of petroleum contaminated soil. Cur Res Green Sustain Chem 2021:100055
Zaynab M, Ml-Yahyai R, Ameen A, Sharif Y, Ali L, Fatima M, Khan KA, Li S (2022) Health and environmental effects of heavy metals. J Kind Saud Univ 34:101653
Zhang T, Lin WB (2014) Metal-organic frameworks for artificial photosynthesis and photocatalysis. Chem Soc Rev 43:5982–5993
Zhang X, Lv L, Qin Y, Xu M, Jia X, Chen Z (2018) Removal of aqueous Cr(VI) by a magnetic biochar derived from Melia azedarach wood. Bioresource Technol 256:1–10
Zhang H, Li XD, Xiao CM, Xie J, Yan X, Wang CH, Zhou YJ, Qi JW, Zhu ZG, Sun XY, Li JS (2022a) Enhanced selective electrosorption of Pb^{2+} from complex water on covalent organic framework-reduced graphene oxide nanocomposite. Sep Purif Technol 302:122147
Zhang S, Liu Y, Ma R, Jia D, Wen T, Ai Y, Zhao G, Fang F, Hu B, Wang X (2022b) Molybdenum(VI)-oxo clusters incorporation activates g-C_3N_4 with simultaneously regulating charge transfer and reaction centers for boosting photocatalytic performance. Adv Funct Mater 32:2204175
Zhang Y, Sun H, Gao F, Zhang S, Han Q, Li J, Fang M, Cai Y, Hu B, Tan X, Wang X (2022c) Insights into photothermally enhanced photocatalytic U(VI) extraction by a step-scheme heterojunction. Research 2022:9790320
Zhang YF, Liu HX, Gao FX, Tan XL, Cai YW, Hu BW, Huang QF, Fang M, Wang XK (2022d) Application of MOFs and COFs for photocatalysis in CO_2 reduction, H_2 generation, and environmental treatment. EnergyChem 4:100078
Zhao G, Li J, Ren X, Chen C, Wang X (2011) Few-layered graphene oxide nanosheets as superior sorbents for heavy metal ion pollution management. Environ Sci Technol 45:10454–10462
Zhao Y, Xu C, Qi Q, Qiu J, Li Z, Wang H, Wang J (2022) Tailoring delicate pore environment of 2D covalent organic frameworks for selective palladium recovery. Chem Eng J 446:136823
Zhong X, Lu Z, Liang W, Hu B (2020) The magnetic covalent organic framework as a platform for the high-performance extraction of Cr(VI) and bisphenol a from aqueous solution. J Hazard Mater 393:122353
Zhou HC, Kitagawa S (2014) Metal-organic frameworks (MOFs). Chem Soc Rev 43:5415–5418
Zhu HX, Liu XY, Jiang Y, Lin DH, Yang K (2022) Sorption kinetics of 1,3,5-trinitrobenzene to biochars produced at various temperatures. Biochar 4:32

Publisher's Note